Earth-Science Reviews 198 (2019) 102933

Contents lists available at ScienceDirect

Earth-Science Reviews

journal homepage: www.elsevier.com/locate/earscirev

Exhumation of west Sundaland: A record of the path of India?

Benjamin Sautter[a,b,*], Manuel Pubellier[a,c], Silvia Králiková Schlögl[d], Liviu Matenco[e], Paul Andriessen[f], Manoj Mathew[g]

[a] Laboratoire de Géologie, Ecole Normale Supérieure, PSL Paris-Sciences-Lettres, Paris, France
[b] Department of Geosciences, Universiti Teknologi PETRONAS, 32610 Bandar Seri Iskandar, Perak Darul Ridzuan, Malaysia
[c] CNRS, UMR8538, France
[d] Department of Geology and Paleontology, Faculty of Natural Sciences, Comenius University in Bratislava, Mlynská dolina, Ilkovičova 6, 842 15 Bratislava, Slovakia
[e] Utrecht University, Department of Earth Sciences, Faculty of Geosciences, Utrecht, the Netherlands
[f] Department of Earth Sciences, Vrije Universiteit Amsterdam, Amsterdam, the Netherlands
[g] South East Asia Carbonate Research Laboratory (SEACaRL), Universiti Teknologi PETRONAS, 32610 Bandar Seri Iskandar, Perak Darul Ridzuan, Malaysia

ARTICLE INFO

Keywords:
Indian Plate
Sundaland
Subduction
Plate migration
Fission tracks
Rifting

ABSTRACT

The Indian Plate commenced its northward migration towards Eurasia in the Early Cretaceous. The lateral effect of this migration on the western edge of the Sunda Plate in Southeast Asia still remains equivocal. In order to assess this effect, we evaluate several key sectors characterized by deep crustal exhumation along a N-S transect from the southern Malay Peninsula to the East Himalayan Syntaxis. The evaluation is aided by a structural analysis of vertical movements and basin development. Five major metamorphic domes with similar geodynamic evolution, maximum P-T burial conditions and exhumation are studied. Exhumation of these domes migrated with time between Late Cretaceous in the Stong Complex (north Malaysia) in the south and Late Miocene in the Gaoligong Shear Zone (south China) in the north, as documented by published work and our new fission track data presented herein. Deformation is characterized by a N-S oriented extension that followed the more regional E-W oriented plate tectonic shortening, creating local core-complexes and *syn*-kinematic magmatism in the footwall of crustal-scale detachments, which displays a consistent temporal northward migration. The N-S extension was associated with the onset of hanging-wall deposition in the sedimentary basins of western Sundaland (e.g. Malay, Sumatra, and Thai Basins) during continuous exhumation of the footwall to upper brittle levels. Our multifaceted analysis of structural and thermochronological data shows a similar succession of tectonic, thermal and sedimentary events in west Sundaland that was driven by the gradual northward migration of India starting from Cretaceous times. We infer that the principal mechanism was driven by the subduction of an excess topography of Greater India rifted continental margin during its underplating, resulting in uplift, thermal anomalies, extensional exhumation and associated subsidence.

1. Introduction

The migration of the Indian Plate towards Eurasia began ~136 Ma ago and the subsequent collision gave rise to the highest mountain range in the world, i.e., the Himalayas (Replumaz and Tapponnier, 2003; Gibbons et al., 2015). Despite extensive studies conducted on this collisional process (e.g., Replumaz and Tapponnier, 2003; Copley et al., 2010; Molnar and Tapponnier, 1977; Patriat and Achache, 1984a,b; Tapponnier et al., 1982; Van Hinsbergen et al., 2011), the evolution of the western edge of the Sunda Plate, during the northward movement of the Indian Plate, is less understood (Ali and Aitchison, 2008; Gibbons et al., 2013; Molnar and Tapponnier, 1977; Patriat and Achache, 1984a,b; Ramkumar et al., 2016, 2017; Williams et al., 2013). Most reconstructions constrain the position of the Indian Plate at least one thousand kilometres away from the western margin of the Sunda Plate during Late Cretaceous - Paleogene times (e.g., Gibbons et al., 2015; Hall, 2002; Replumaz and Tapponnier, 2003; Zahirovic et al., 2014), while, other studies infer a coupling between the two plates (e.g., Ali and Aitchison, 2008; Pubellier et al., 2001; Replumaz et al., 2004; Socquet and Pubellier, 2005).This disparity in theories shows that the crustal nature and lateral extent of Greater India are topics that are yet to be satisfactorily resolved (Ali and Aitchison, 2005; Klootwijk et al., 1992; Müller et al., 2000; Van Hinsbergen et al., 2011). In other words, during the Late Cretaceous to Early Paleogene migration of the Indian Plate towards Eurasia, the thinned continental part of Greater India may have been in tectonic-contact with the western margin of the

* Corresponding author at: Geosciences Department, Universiti Teknologi PETRONAS, 32610 Bandar Seri Iskandar, Perak, Malaysia.
E-mail address: benjamin.sautter@utp.edu.my (B. Sautter).

https://doi.org/10.1016/j.earscirev.2019.102933
Received 20 September 2018; Received in revised form 8 August 2019; Accepted 20 August 2019
Available online 25 August 2019
0012-8252/

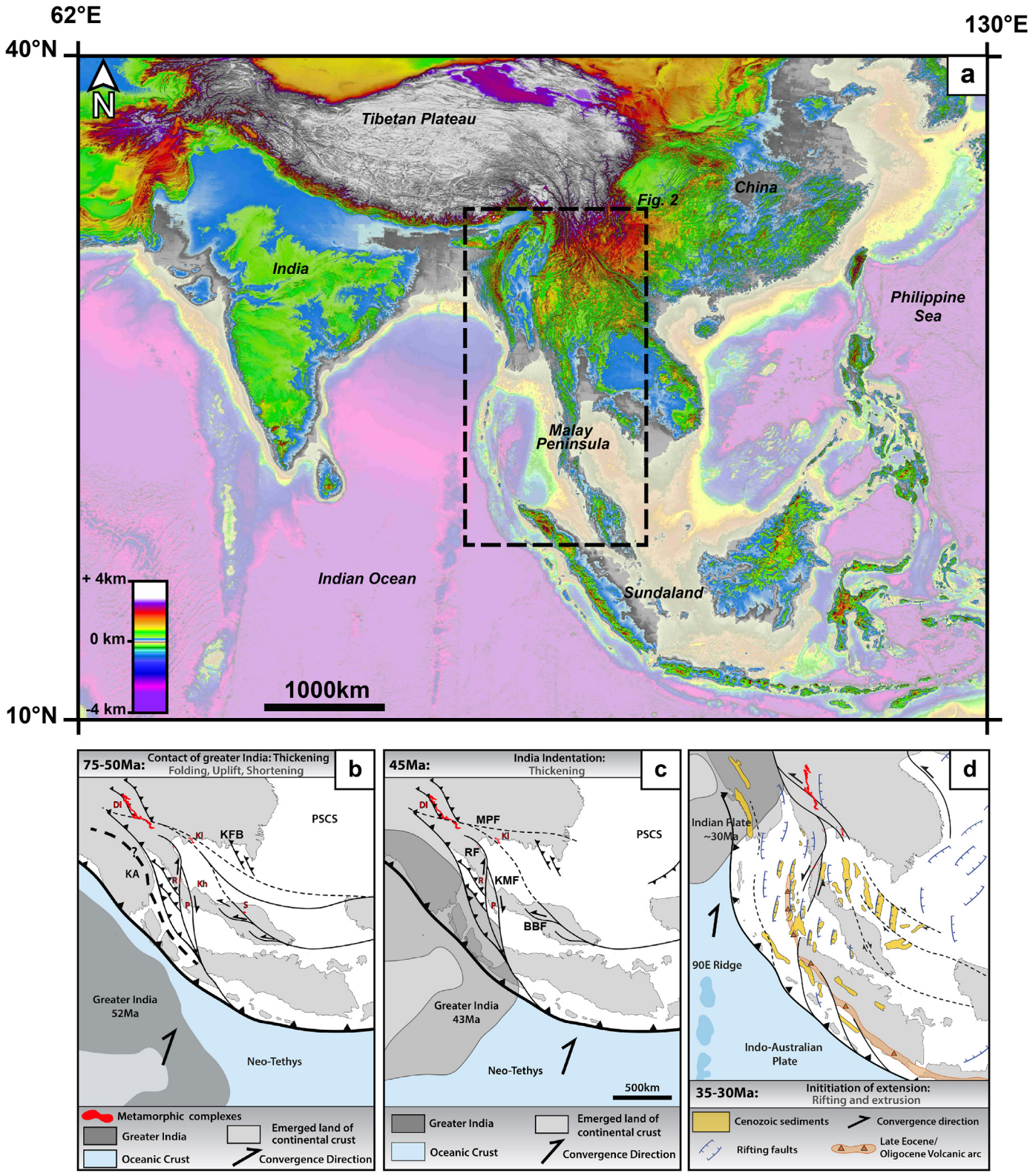

Fig. 1. a) Topographic map of SEASIA based on Digital Elevation Model (GTOPO + GEBCO), the dash line square represents the study area; b) c) d) reconstructions modified from Sautter et al., (2017) at and 75-50 Ma (b), 45 Ma (c) and 35 to 30 Ma(d). BBF. Bok Bak Fault; DI. Doi Inthanon; KA Kohistan Arc; KFB: Kampot Fold Belt; Kl. Klaeng Fault Core; KMF. Khlong Marui Fault; MPF. Mae Ping Fault; P. Khao Phanom ductile core; PSCS. Proto South China Sea; R. Ranong ductile core; RF. Ranon Fault; S. Stong Complex;

Sunda Plate (Fig. 1) (Sautter et al., 2017; Bertrand et al., 1999; Morley, 2012; Curray, 2005; Hall, 2002; Lacassin et al., 1997). An enhanced tectonic coupling is observed through the activity of large-scale strike-slip faults (e.g., Ranong, Khlong Marui, Bok Bak Fault, Mae Ping Fault, Figs. 1b and c) and large-wavelength folds, which resulted in the emplacement of magmatic intrusions. The ensuing crustal thickening was accompanied or followed by the formation of a number of metamorphic domes, such as Stong, Khanom, Khlong Marui, Ranong, Klaeng,

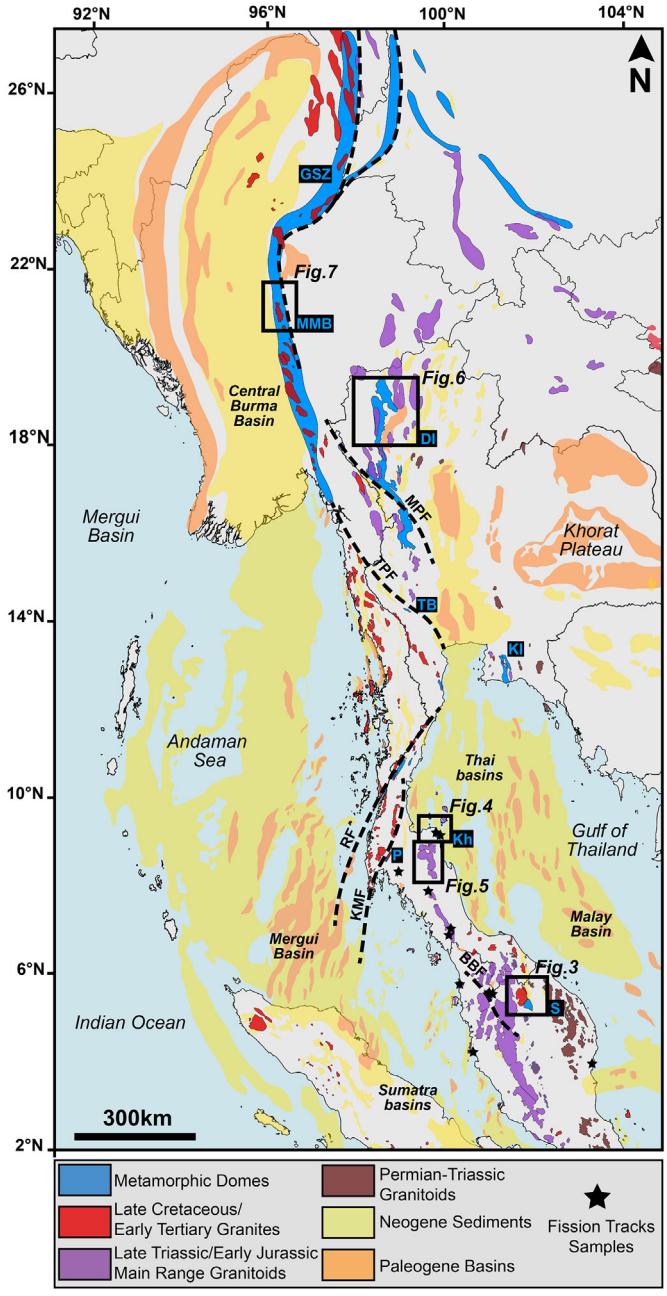

Fig. 2. Map of the study area showing the main features described in the paper. The black square boxes represent the location of following figures further in the paper. The metamorphic complexes are represented in blue: from south to north, S: Stong, P: Phanom, Kh: Khanom, Kl: Klaeng, TB: Thabsila, DI: Doi Inthanon, MMB: Mogok Metamorphic Belt. (For interpretation of the references to colour in this figure legend, the reader is referred to the web version of this article.)

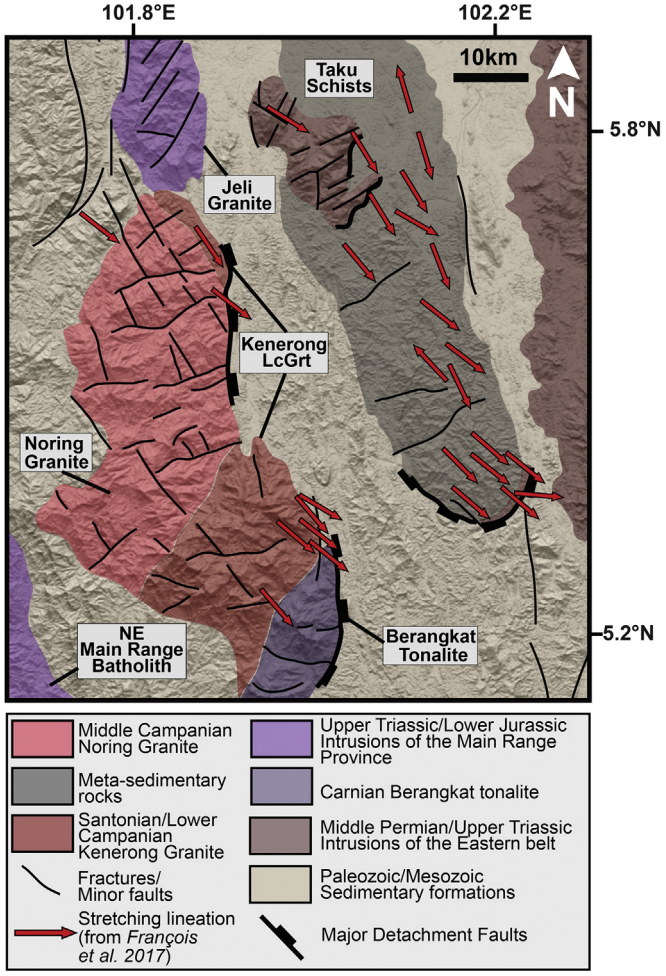

Fig. 3. Structural map of the Stong Complex showing the different metamorphic and magmatic units involved in the deformation.

Khabila, Doi Inthanon, and Mogok/shan scarp, which are often attributed to extensional detachments (or large normal faults) and major strike-slip displacements (Figs. 1b and 2) (e.g., Bertrand et al., 1999; Gardiner et al., 2016; Macdonald et al., 2010; Watkinson et al., 2011; Zhang et al., 2012a).

We analyse the exhumation of the western part of Sundaland with an explicit focus on understanding the mechanisms involved in the formation of metamorphic domes. In order to understand the regional structural context with emphasis on vertical movements required to derive a coherent tectonic scenario for the northward motion of the Indian Plate, we integrate previously published geochronological and structural data from the Malay Peninsula in the south to the Gaoligong Shear zone in the north with our newly acquired zircon and apatite fission track data from the critical area of the Khanom dome of southern Thailand (Fig. 2). The results are discussed in the geodynamical context of SE Asia evolution.

2. Metamorphic complexes of west Sundaland

Several metamorphic domes have been documented along the western margin of Sundaland (Fig. 2) (e.g., Ali et al., 2016; Bertrand et al., 1999; Kawakami et al., 2014; MacDonald et al., 1993; Morley, 2012; Zhang et al., 2012a). Most of them are located within a N-S oriented chain of Mesozoic intrusions. We will further analyse and discuss these metamorphic domes in their geographical order starting from Peninsular Malaysia in the south to northeastern Myanmar.

The southernmost Stong metamorphic core-complex (Figs. 2 and 3) is made up of Paleozoic sediments and magmatic rocks buried and metamorphosed up to amphibolite facies (the Taku Schist) during the Permo-Triassic Indosinian Orogeny. They were subsequently exhumed in the Late Cretaceous along a large offset top-SE to SSE detachment associated with *syn*-kinematic magmatism intruding its footwall (the Taku-Stong detachment of Ali et al., 2016; François et al., 2017). This magmatism resulted in two Late Cretaceous intrusions, Kenerong and Noring, emplaced at around 84 Ma and 75 Ma, respectively (Bignell and Snelling, 1977; Cobbing et al., 1986; Ng et al., 2015a). The Kenerong pluton was emplaced in the early stages of the core-complex evolution and is a ductile-sheared biotite leucogranite with several generations of

foliated leucogranite veins, aplites and pegmatites intruding the metamorphic host rocks (Fig. 3) (François et al., 2017; Ghani, 2009). The Noring pluton is a relatively undeformed granite with large K-feldspar phenocrysts that lacks a pervasive foliation in its core and is affected by brittle shear zones along its eastern margin. It was emplaced at pressures of ~2–3 kbar during the late stages of the core-complex evolution (Ghani, 2000). The Late Cretaceous deformation includes the formation of a shearing foliation and folding of the host rock, which was affected by metasomatism, veining and migmatitization during the syn-kinematic emplacement of granites (François et al., 2017). The mylonitic core-complex foliation in the Taku Schist and Stong structure displays top-SE to SSE stretching lineations with clear shear bands and kinematic indicators (sigma clasts), affected by the metasomatic growth of hornblende, andalusite and sillimanite (Ali et al., 2016; François et al., 2017). These studies have documented a Late Cretaceous to Paleogene exhumation age (~72–55 Ma) of the core-complex by integrating previous high-temperature thermochronology data with low-temperature zircon fission-track dating. Apatite fission track ages (~45–30 Ma) inferred a subsequent exhumation event at lower temperatures that was interpreted to have been associated with another extensional event during Eocene/Oligocene times.

Southeast of Surat Thani in Thailand, the 20 km wide, NW–SE oriented, Khanom dome is located near the shoreline of the Gulf of Thailand (Figs. 2 and 4a). This dome is characterized by several magmatic and metamorphic units. The petrography and mineralogy of these units have been studied by Kawakami et al. (2014), together with an in-situ LA-ICP-MS U—Pb dating of zircons and a CHIME study on monazite. The complex is bordered by two WNW–ESE oriented faults; the Khanom Fault in the north and the Sichon Fault in the south (Kawakami et al., 2014; Kosuwan, 1996) (Fig. 4a). The core of the dome is composed of Ordovician granite that was partly recrystallized during a Late Triassic Indosinian thermal event. This event is interpreted to be driven by the magmatic emplacement of S-type Main Range granites of Peninsular Malaysia, together with one other possible Paleogene cooling event dated from the rims of monazites (Kawakami et al., 2014). An additional granitic pluton intruded the dome in the Late Cretaceous (67.5 ± 1.3 Ma, Fig. 4a), while the remainder of the massif is composed of meta-sedimentary rocks. All these rocks were affected by a Late Cretaceous to Paleocene metamorphic event that included metasomatism associated with the coeval plutonic intrusion. To elaborate, the 72 ± 13 Ma Haad Nai Phlao gneiss (Kawakami et al., 2014) contains a biotite and sillimanite assemblage and is pervasively affected by a N-S oriented stretching lineation with a top-S sense of shear. Clear kinematic indicators can be observed in the field, such as along the southern end of the Nai Phlao beach (location 144, Fig. 4a), a migmatitic gneiss is affected by a clear top-S sense of shear (Fig. 4b, c and d). The 66 ± 9 Ma Laem Thong Yang porphyroblastic biotite gneiss (Kawakami et al., 2014), is exposed further south on the eastern side of the Khanom dome (stop 145 in Fig. 4). This augen-gneiss is strongly foliated and folded together with other leucogranite bodies (Sautter et al., 2017).

As observed at stop 149 (Fig. 4a), the Khao Yoi schist has a

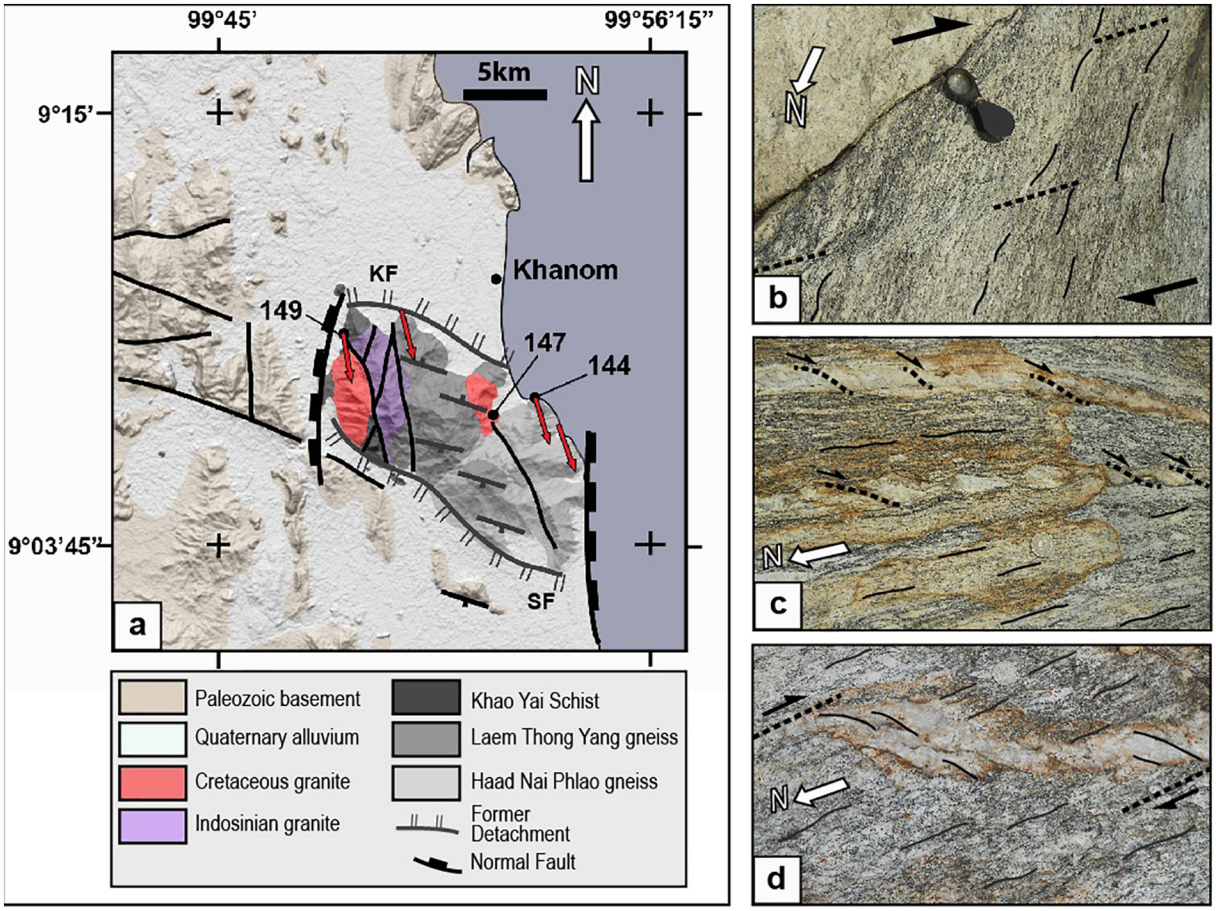

Fig. 4. a) structural map of the Khanom Dome (modified from Sautter et al. 2017); The red arrows represent the stretching lineation seen in the field, at four different locations. The four black dots are the stops described in the text. b,c,d: field photographs at the location 144 on the eastern side of the Khanom dome. The Haad Nai Phlao gneiss is locally affected by high temperature migmatitization and shows evidence of dextral shear in present day orientation in successive stages of deformations. b: C—S bands showing a top-to-the-west dextral shear. Scale is given by the black lenses. c: quartz veins boundinage with a top-to-the-west dextral shear. d) Tension gash filled with quartz showing a top-to-the-south dextral shear. (For interpretation of the references to colour in this figure legend, the reader is referred to the web version of this article.)

conspicuously stretched cigar-shaped structure, with N-S stretching lineation associated to a regional E–W shortening (Figs. 4 and 6 of Sautter et al., 2017). This schist contains a meta-sedimentary assemblage of dominantly quartz schists that are cross-cut by leucogranitic intrusions with a foliation parallel to that of the meta-sediments. The P–T conditions were estimated to be 500–650 °C from 2 to 5 kbar (Kosuwan, 1996). To the west of the Khanom dome, the Khao Phanom ductile core (Fig. 2, P) experienced a major exhumation that started in the Lower Eocene due to transpressional shearing along a restraining bend created by the Khlong Marui Fault (Kanjanapayont et al., 2012; Watkinson et al., 2008, 2011). 50 km north of the Khlong Marui fault, several other ductile cores are observed along a similar shear zone (the Ranong Fault, Fig. 2), which were affected by successive transpressional episodes from the Late Cretaceous to the Late Eocene, as noted by Watkinson et al. (2011). According to these authors, during the Middle Eocene (~44 Ma), major dextral shearing occurred in ductile conditions following two earlier right-lateral stages in the Late Cretaceous and Late Paleocene to Lower Eocene (59–49 Ma). Deformation was associated with magmatism between ~81 Ma and 71 Ma and at ~48 Ma.

The overall E–W direction of compression is also documented in brittle conditions in other areas of Peninsular Thailand. South of the Khanom dome, this direction of compression is observed in the granites of the Late Triassic/Lower Jurassic Main Range province and Cambro-Ordovician to Permo-Carboniferous sedimentary formations (Figs. 2 and 5). The sediments are folded along N−S oriented lineaments that surround the plutons and follow the dome edges. Indeed, the bedding traces rarely appear cross-cut by the plutons, suggesting a post-intrusion deformation (Fig. 5). Nonetheless, the plutons are deformed by conjugate brittle fractures striking NW–SE and NE–SW, which is otherwise widely observed elsewhere along the Malay Peninsula (Sautter et al., 2017). These folds and fractures suggest an overall E-W oriented compression and at a later stage, are cross-cut by large offset E–W striking normal faults (Fig. 5). Predominantly, these faults dip southward along the gradually-decreasing topographic gradient of the Malay Peninsula. This extensional deformation is compatible with the numerous E–W tensional joints cross-cutting the N−S ductile fabric of the northern-located Khanom dome (Sautter et al., 2017). Overall, these observations indicate that the deformation was characterized by ductile strike-slip shear with an E-W oriented shortening and was followed by a N−S extension with a dominant top-S sense of shear.

To the north of the Gulf of Thailand, the Nong Yai gneiss localized in the Klaeng Fault zone (Figs. 1c and 2) was intruded by a leucogranite at 78.6 ± 0.7 Ma followed by a second intrusion at 67 ± 1 Ma to 72.1 ± 0.6 Ma (Kanjanapayont et al., 2013). These magmatic rocks together with older gneissic rocks are affected by NNW–SSE to NW–SE oriented ductile sinistral shearing in the Klaeng Fault zone that may have been responsible for significant Eocene exhumation (Kanjanapayont et al., 2013).

The Doi Inthanon metamorphic core complex (Figs. 2 and 6) is located in NW Thailand and experienced a complex polyphase deformation. Two major episodes of metamorphism postdate the Indosinian Orogeny viz., 1) a thermal event associated with magmatic emplacement from ~84 Ma to 72 Ma (Late Cretaceous), followed by, 2) prograde metamorphism during Eocene to Oligocene crustal thickening (Dunning et al., 1995; Gardiner et al., 2016). The final exhumation of the dome occurred in the Miocene via a low angle extensional detachment (Gardiner et al., 2016). In the core complex footwall, the P-T-t path shows retrograde metamorphic conditions at 78 Ma followed by continuous exhumation during Cenozoic times (Macdonald et al., 2010).

The Doi Inthanon dome extends further north of the Doi Suthep metamorphic dome (Fig. 6). The latter appears as a NNW–SSE striking dome, comprising of amphibolite-grade migmatitic gneisses separated by lower grade mylonites within a metasedimentary sequences (Gardiner et al., 2016; Rhodes et al., 2000). The dome has also been affected by a polyphase deformation recorded from the Indosinian

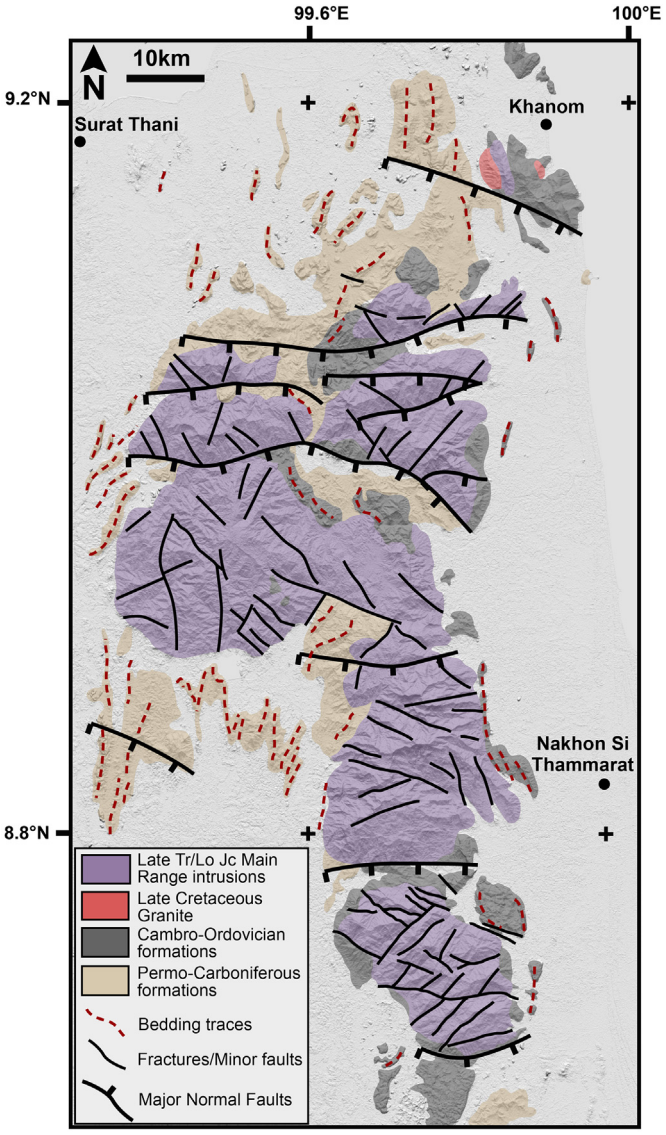

Fig. 5. simplified structural map of Central Peninsular Thailand highlighting the deformation of the non-metamorphic basement rocks. Conjugate fractures in the post-Indosinian granites (in purple) and N-S bedding traces of sedimentary formations (in red). (For interpretation of the references to colour in this figure legend, the reader is referred to the web version of this article.)

Orogeny in the Triassic until the Middle Miocene rifting of the nearby Chiang Mai Basin (Fig. 6) (Gardiner et al., 2016; Morley et al., 2011; Rhodes et al., 2000). The Indosinian event was associated with the onset of extensive magmatism observed in the protholith of an orthogneiss deformed by subsequent tectonic events (Gardiner et al., 2016). A Cretaceous thermal overprint is interpreted by Gardiner et al. (2016) as regional metamorphism related to the subduction of the neoTethys before the Himalayan collision. However, the author interpreted a main prograde metamorphic event to have occurred in the Late Eocene–Oligocene by inducing partial melting of zircons and monazite. This event was followed by a top-E activation of an extensional detachment associated with a Miocene exhumation that was coeval with the rifting of the Chiang Mai Basin along N−S oriented normal faults. Other studies have interpreted the different stages of metamorphism to represent a single retrograde P-T-t metamorphic path from a high grade Indosinian event to brittle extension in the Miocene (Macdonald et al., 2010). Essentially, the Doi Suthep complex is part of the Doi Inthanon Complex by forming a dome structure bounded by an extensional detachment with a SE antiformal plunge and an apparent top-E sense of

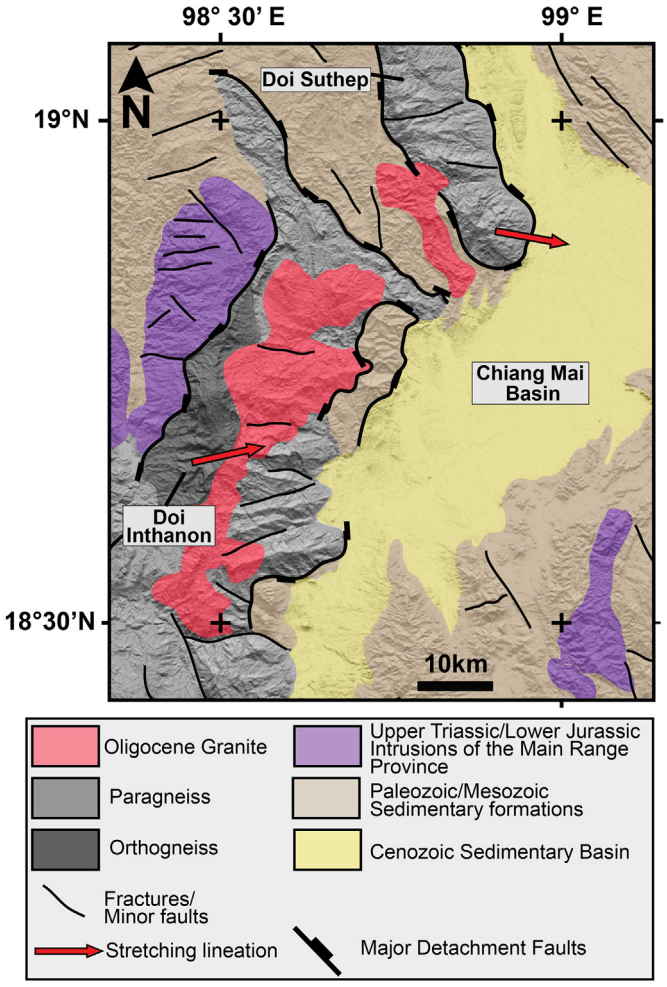

Fig. 6. structural map of the Doi Inthanon (DI) and Doi Suthep (DS) complexes. Ductile shear senses are represented by red arrows. (For interpretation of the references to colour in this figure legend, the reader is referred to the web version of this article.)

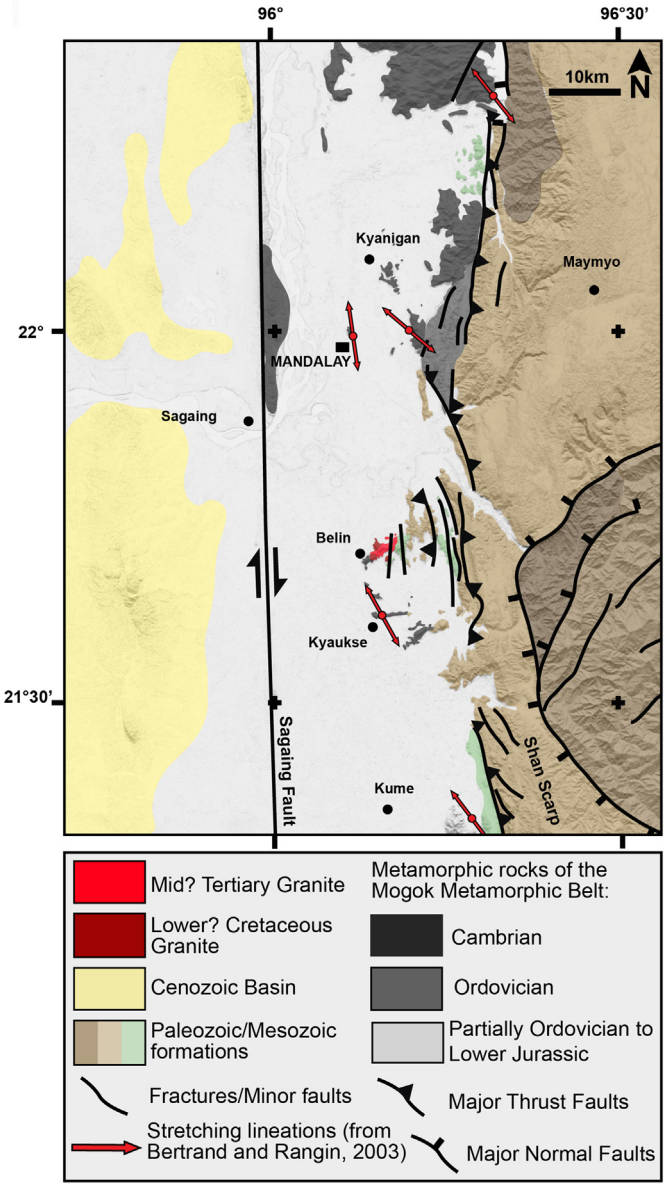

Fig. 7. structural map of the Mogok Metamorphic Belt. Stretching lineations are represented with red arrows. (For interpretation of the references to colour in this figure legend, the reader is referred to the web version of this article.)

shear observed in the mylonitic gneisses (Fig. 6, see also Rhodes et al., 2000).

Further northwest in Myanmar, a younger shear zone was evidenced by NNW–SSE stretching lineations (red arrows in Fig. 7), where the last age of metamorphism in the Mogok Metamorphic Belt was constrained between ~26 Ma in the south and ~21 Ma in the north (Bertrand et al., 1999; Socquet and Pubellier, 2005), or from ~30 Ma to 15 Ma between 18°N and 23°N (Bertrand et al., 2001). The extension and associated exhumation in the Mogok belt are interpreted to be derived from the northward migration of East Himalayan Syntaxis during the Oligocene - Middle Miocene (Bertrand et al., 2001). Furthermore, Searle et al. (2007) highlighted the complex history of metamorphic episodes that affected the Mogok-Shan Scarp complex from the Paleozoic until the recent dextral shear of the Sagaing Fault (Fig. 7). They described a metamorphic event in the Middle Eocene resulting in the crystallization of metamorphic monazite at sillimanite grade and the growth of zircon rims between ~47 Ma and 43 Ma (Searle et al., 2007). This metamorphic assemblage suggests HT sillimanite + muscovite with a peak at 680 °C and 4.9 kbar. A *syn*-metamorphic melting generated leucogranites with garnet and tourmaline at 45.5 ± 0.6 Ma and 24.5 ± 0.7 Ma, which implies another metamorphic equilibrium around 606–656 °C and 4.4–4.8 kbar at 29.3 ± 0.5 Ma (Searle et al., 2007).

The Gaoligong Shear Zone marks the boundary of the southeastern Tibetan Plateau, south of the Three Rivers region (Fig. 2). The elevation decreases from the north to the south across a steep topographic gradient, where several E–W valleys can be observed that are likely the result of recent major strike slip faulting. Significant shearing took place during Oligocene – Miocene times and this is interpreted to be driven by the northward motion of India (Huang et al., 2015; Zhang et al., 2012). Metamorphic rocks along the shear zones are re-folded in large antiforms affecting earlier Indosinian tight folds, as noted by Zhang et al. (2012). These authors suggest that a stage of ductile shear ended during the Late Miocene as recorded by mica $^{40}Ar/^{39}Ar$ ages of mylonites of ~15–16 Ma, together with leucogranites and proto-mylonites of ~10–12 Ma. A high-grade metamorphism consisting of amphibolite, migmatites, garnet–biotite–sillimanite gneiss, marbles, and garnet-bearing leucogranite veins was interpreted to reflect the Indosinian orogeny (Zhang et al., 2012). Strongly deformed gneisses with sub-horizontal stretching lineation formed a dome-shaped structure oriented NNW-SSE, where shear bands in vertical folded leucogranite veins in biotite, garnet and sillimanite gneisses show dextral transpression (Huang et al., 2015). A thermochronological study analysing

orthogneisses and mylonites in the southern Gaoligongshan revealed a stage of mylonitization between ~19 and 12 Ma (Eroğlu et al., 2013). An apatite fission track study from the Gaoligong shear zone has revealed exhumation ages between ~8.4 and 0.9 Ma (Wang et al., 2008), interpreted to be the result of block rotations leading to differential uplift (see also Socquet and Pubellier, 2005).

All these observations along the western margin of the Sundaland tectonic unit show high grade metamorphic rocks occurring as domes across the Yanshanian magmatic arc, and along large-scale strike-slip faults. Often referred to as metamorphic core complexes due to the presence of large normal detachment faults and syn-kinematic plutons intruding their footwalls, these domes appear to develop in the same structural setting and P–T conditions. These metamorphic domes are oriented N−S to NW–SE and are affected by intense stretching lineation that generally shows top-S to SSE senses of shear, with the notable exception of the Doi Inthanon dome (including the Doi Suthep structure), where the shearing is top-E. In most situations, amphibolite-grade metamorphic conditions were recorded at the peak of burial or thermal overprint. Deformation was also associated with E-W oriented compression evidenced by N-S oriented large-scale folds together with NW-SE and NE-SW conjugate fractures in the granitic plutons. Deformation migrates with time, with younger ages northwards. A single conventional block accretion cannot explain the reviewed metamorphic events because the deformation is diachronous.

To achieve a complete understanding of exhumation along all these metamorphic domes through time, we combined existing and newly acquired thermochronological data along the western Sundaland margin.

3. Fission track thermochronology

3.1. Documented thermochronological records of western Sundaland

Several studies have been previously conducted to better constrain the emplacement and subsequent vertical motions of magmatic bodies across the Peninsular Malaysia and Thailand (e.g., Hutchison, 1977; Ng et al., 2015a and Ng et al., 2015b). By analysing the petrology, mineralogy, and chemical composition of granites from different magmatic belts, these authors have also established the relative depths of magmatic emplacement. Crystallization ages were established through different methods of radioactive decay, such as U−Pb, K−Ar, $^{40}Ar-^{39}Ar$, and Rb−Sr dating, while ages of exhumation, whether it is due to tectonics, erosion or isostatic compensation, were obtained by low-temperature thermochronology, such as zircon and apatite fission track analysis (ZFT, AFT), and (U−Th)/He dating of zircon and apatite (ZHe and AHe). Granitoids from the Permian to Triassic volcanic arc in east Peninsular Malaysia have a rather porphyric texture with alkaline feldspars (orthoclase and microcline). The surrounding sedimentary rocks are metamorphosed, and inclusions/enclave of volcanic rocks are often present in the granites (Ismail et al., 2003). Metamorphic aureoles are also observed (Hutchison, 1977). Hence, the east Malaysian granites are considered as epizonal, indicating that they were emplaced in the upper part of the continental crust. The noticeable lack of large amounts of cassiterite is also an argument for superficial crystallization (Hutchison, 2013). By comparison, the granites from the Late Triassic/Early Jurassic Main Range Province show different characteristics and are considered as mesozonal (Hutchison, 1977). No metamorphic aureoles are seen except for a few skarns in the limestone (e.g., the Kinta Valley), and they are defined by a porphyric texture with feldspar phenocrysts.

The emplacement of granitoid bodies of the Main Range Province (batholith and side plutons) occurred around ~200 Ma, documented by muscovite and biotite K−Ar dating and zircon U−Pb dating (Krahenbuhl, 1991; Seong, 1989; Tai Seong and Seong, 1990), while more recent studies have shown a westward migration towards younger ages (Ng et al., 2015b; Ng et al., 2015a). In the western part, cooling of some of the isolated plutons (Kledang and Bujang Melaka) through ~320–200 °C (zircon partial annealing zone, ZPAZ, Tagami et al., 1998) was documented between ~120 and 80 Ma; whereas, the plutons from the Main Range Batholith cooled through the ZPAZ between ~80 and 60 Ma (Krahenbuhl, 1991). Between ~30 and 20 Ma, all plutons crossed the apatite partial annealing zone (APAZ; ~120–60 °C; e.g., Wagner and van den Haute, 1992). Overall, all Main Range post-Indosinian plutons seem to follow a similar trend from their emplacement at ~200 Ma until their late stages of exhumation, which is different in isolated plutons (~100 Ma) and the Central Batholith (~70 Ma). The exposed areas of the Central Batholith represent deeper parts of the entire magmatic province that suffered larger amounts of exhumation as compared to the isolated plutons. Sigmoid duplexes observed in the midst of the batholith, resemble large C/S bands (Sautter and Pubellier, 2015) and are in favour of this hypothesis. A major exhumation event occurred between ~100 Ma and 70 Ma as inferred by an increase of cooling rates in this granitoid province (Cottam et al., 2013; Krahenbuhl, 1991).

According to Fyhn et al. (2016), the internal zones of the Cambodian Kampot Fold Belt (Fig. 1b) revealed ZFT ages of ~80–60 Ma, whereas older ZFT ages of ~150–110 Ma and ~100–80 Ma were documented in the external zones. Most of AFT data passed through the APAZ during ~25–15 Ma, except samples that document older exhumation event(s) dated at ~40–35 Ma, and ~60–55 Ma (Fyhn et al., 2016).

In Peninsular Thailand, only scarce AFT data exist. However, they show a similar exhumation trend between ~20 and 30 Ma (Putthapiban, 1992; Upton, 1999; Upton et al., 1997). The region around Phuket Island shows few ZFT and TFT (titanite) ages centred at ~55 Ma (Putthapiban, 1992) and numerous other AFT data centred at ~20 Ma (Blomme, 2013). Further northwards, AFT data from continental formations of the Khorat Plateau show older ages, clustered around ~50 Ma (Racey et al., 1997). According to these authors, sedimentary rocks have not been buried deep enough after ~50 Ma to reset their thermochronological clock and have been subjected to a strong uplift in the Paleocene. In southern Peninsular Thailand, the emplacement of the Thai Batholith (Nakhon Si Thammarat Range in Fig. 5) is synchronous to those from the Main Range in Malaysia (Beckinsale et al., 1979; Charusiri et al., 1993; Schwartz et al., 1995). However, no FT data are available to date.

In order to constrain the history of vertical motions of the entire Peninsular Malaysia and Thailand, we conducted a fission-track analysis of 11 samples from the Main Range granites located in northwestern Malaysia and southern Thailand. The results show FT ages that range from ~32 Ma to 69 Ma for zircon and from ~16 Ma to 25 Ma for apatite. Among these samples, two yielded results that are relevant for the study area.

3.2. ZFT and AFT dating of the Khanom Dome

Two samples of the Khanom core complex (stops 145 and 147 on Fig. 4a, locations and analytical results in Tables 1 and 2) yielded reliable results for the studied area.

The first sample is a foliated granite located on the eastern flank of the dome (stop 145), mapped as the Haad Nai Phlao gneiss by Kawakami et al. (2014), which is a sillimanite and garnet bearing muscovite-biotite gneiss (Kosuwan, 1996). The gneiss is cut by pegmatites and aplites of large crystals of K-Feldspar and muscovite, locally interlayered with calc-silicate rocks. At the same location, we observed and sampled a biotite-granite with feldspar phenocrysts as large as 5 cm. FT analysis on this sample (stop 145, Fig. 4a) yielded ZFT central age of 33.5 ± 1.4 Ma and AFT central age of 24.6 ± 1.1 Ma (Tables 1 and 2). Both ZFT and AFT ages passed the chi-squared probability test ($P(\chi 2) > 5\%$; Galbraith (1981)), indicating that all grains in each sample belong to one homogeneous age population.

Sample 147 (stop 147) was taken from the northern flank of the

Table 1
Results of the zircon fission track analysis on the two samples from the Khanom dome performed for this study.

Zircon Fission Track analytical data from the Khanom Dome, Thailand.

Sample	coordinates	Rock-type	Mineral assemblage	Geochemistry	Number of grains	ρ_d 10^6tr/cm^2 (N_d)	ρ_s 10^6tr/cm^2 (N_s)	ρ_i 10^6tr/cm^2 (N_i)	P(χ^2) (%)	Age dispersion (%)	Fission track age (Ma)
145	9°06′52.5″N 99°53′55.5″E	Main Range Granite Gneiss	Biot	S-Type	10	0.50919 (10513)	7.1429 (1988)	6.9237 (1927)	100	0.00	33.5 ± 1.4
147	9°06′43.1″N 99°52′15.9″E	Late Cretaceous Granite	Biot	?	9	0.50919 (10513)	5.1385 (1269)	5.0737 (1253)	100	0.00	32.9 ± 1.6

dome, from the relatively undeformed Khao Pret Cretaceous granite, which includes large pegmatitic veins of leucogranites (Kawakami et al., 2014). FT analysis revealed a ZFT age of 32.9 ± 1.6 Ma and an AFT age of 17.9 ± 1.1 Ma (Tables 1 and 2). Both ZFT and AFT ages passed the chi-squared probability test (P(χ2) > 5%; Galbraith, 1981)), indicating that all grains in each sample belong to one homogeneous age population.

In order to quantify fluorine and chlorine contents of the apatite specimens, the Dpar values were measured as well. Both apatite samples (stops 145, 147) displayed the same range of Dpar values, between 1.9 and 2.4 µm, indicating fairly similar chemical compositions and relatively fluorine-rich apatites (Burtner et al., 1994) with a low resistance to annealing (Ketcham et al., 1999).

Due to the low number of confined horizontal tracks in sample 147, modelling of thermal history was possible only for sample 145 (Fig. 8a). The track length distributions of confined horizontal tracks is unimodal with negative skewness with increased standard deviation (typically > 2 µm) (Fig. 8b). Such track length distribution is indicative for basement rocks with slow cooling or prolonged residence in the APAZ (~60–120 °C; e.g., Wagner and van den Haute, 1992). Thermal history of sample 145 was modelled using HeFTy® programme (Ketcham, 2005) and multi-kinetic annealing model of Ketcham et al. (2007). The thermal modelling of the Khanom core complex revealed a fast cooling from the Late Eocene to the Late Oligocene (36–26 Ma) with a rate of 23 °C/Ma. Such fast cooling likely reflects a strong tectonic-controlled exhumation. This fast cooling event terminated in the Late Oligocene and was followed by a lower moderate cooling or prolonged residence in the APAZ from ~27 Ma to 22 Ma with a rate of ~12 °C/Ma (Fig. 8a). In addition, the AFT age indicates a Miocene continued cooling up to present-day temperatures with rates lower than 2 °C/Ma. Such low cooling rates most probably reflect pure erosional unroofing processes (Boettcher and Milliken, 2009; Portenga and Bierman, 2011).

4. Discussion

Our compilation of thermochronological and geological data reveals a northward younging of the metamorphism, exhumation and rifting ages (Fig. 9, Table 3). The data were selected from the Stong, Khanom, Doi Inthanon, Thabsila, and Mogok metamorphic complexes (Fig. 2). Dating of nearby early basin-fills were taken from literature (e.g., Gardiner et al., 2016; Heward et al., 2000; Madon and Mansor, 1999; Mansor et al., 2014; Morley, 2016; Morley and Racey, 2011; Nantasin et al., 2012; Polachan and Racey, 1994; Srisuriyon and Morley, 2014; Zhang et al., 2012). We plotted the evolution of metamorphism, exhumation and infilling of early rifted Tertiary basins with time versus latitude (Fig. 8). The results show a clear chronology of successive events; 1) HT metamorphic event, 2) post-kinematic intrusions, 3) exhumation, and 4) rifting; that is common for each sector analysed in this paper.

4.1. A HT metamorphic event

All metamorphic core complexes occur in the same temperature conditions (600 °C) and structural settings, being affected by pervasive top- S to SSE stretching lineations in most locations. High temperature (amphibolite facies) metamorphic conditions have been evidenced with the occurrence of sillimanite, garnet, or hornblende minerals. Moreover, a south to north younging of the metamorphic ages is witnessed. We see a clear linear northward trend of the metamorphic ages from northern Malaysia in the Late Cretaceous to Gaoligong, China, in the Middle Miocene. By the end of this metamorphic event, a thermal anomaly is recorded in all the western regions of the Sunda Plate, represented by undeformed isolated plutons that crosscut the deformation.

4.2. Late stage post-kinematic intrusions

Thermochronological studies have highlighted numerous occurrences of Late Cretaceous to Tertiary isolated intrusions along the Malay Peninsula (Beckinsale et al., 1979; Charusiri et al., 1993; Cobbing et al., 1986; Cottam et al., 2013; Gardiner et al., 2015; Ghani et al., 2013; Krahenbuhl, 1991; Kwan et al., 1992; Ng et al., 2015a, 2015b; Schwartz et al., 1995; Searle et al., 2012). The geodynamic setting driving these intrusions over a wide region is not always well understood, and the reasons for the thermal anomaly highlighted by many authors remain unexplained (Cottam et al., 2013; Ghani, 2009; Morley, 2012).

A geochemical study of the different granitic belts of Peninsular Malaysia evidenced a uniform negative anomaly rare earth elements (i.e., europium) in the Main Range Province; whereas, the Late Cretaceous isolated plutons show no such anomaly compared to the Late Paleozoic granitoids, indicating a primitive mantle source (Hassan and Hamzah, 1998). Because these plutons are localized along the southern part of the Bentong Raub Suture Zone, the presence of a crustal dislocation that was reactivated in a post-orogenic setting has been inferred (Hutchison, 1977). However, the widespread occurrence of such thermal anomalies across the Sundaland margin makes it difficult to be explained as a local phenomenon. Furthermore, the emplacement age of plutons is found to be younging northwards (Fig. 9).

Seismic tomography studies in western Sundaland have showed deep rooted thermal anomalies (Pesicek et al., 2008). By following examples from the subduction of the East Pacific Rise (EPR) beneath the Gulf of California, Pesicek et al. (2008), interpreted a bended Tethysian slab, presently at depths between ~250 and 530 km, beneath the southern Malay Peninsula. Temporal reconstructions of the age of the subducted Tethyan lithosphere revealed the presence of a slab window beneath Java and south Sumatra in the Early Paleogene (Whittaker et al., 2007). According to these authors, such an event implying a mantle rise in the upper plate lithosphere would have enhanced the active rifting in the Java Sea Region and the continuation of extension between ~50 Ma and 35 Ma in Sumatra, owing to low viscosities of the mantle wedge. However, this interpretation is in contrast with more

Table 2
Results of the apatite fission track analysis on the two samples from the Khanom dome performed for this study.

Apatite fission track analytcal data from the Khanom Dome, Thailand.

Sample	Coordinates	Rock-type	Number of grains	ρ_d 10^6tr/cm^2 (N_d)	ρ_s 10^6tr/cm^2 (N_s)	ρ_i 10^6tr/cm^2 (N_i)	P(χ^2) (%)	Age dispersion (%)	Dpar measured (# Dpar)	Mean track length (μm) (# lengths)	Std (μm)	Fission track age (Ma)
145	9°06′52.5″N 99°53′55.5″E	Main Range Granite Gneiss	15	1.0102 (20857)	0.6646 (977)	4.8837 (7179)	100	0.00	1.97–2.41 (80)	13.17 ± 0.19 (91)	1.83	24.6 ± 1.1
147	9°06′43.1″N 99°52′15.9″E	Late Cretaceous Granite	15	1.0102 (20857)	0.2509 (359)	2.5287 (3618)	100	0.00	1.93–2.57 (76)	14.16 ± 0.39 (9)	1.82	17.9 ± 1.1

recent geometries showing a modified position of the slab window with time (Fabian and Whittaker, 2010). By comparing several tomographic models of the region, these authors showed that the Tethyan slab window was located beneath south Sumatra and the north Malay Peninsula between ~69 Ma and 43 Ma (Fabian and Whittaker, 2010). Through a restoration of the subducted magnetic isochrons and fracture zones of the northern Wharton Basin, Jacob et al. (2014), also evidenced an Early Cenozoic slab window in the Andaman Sea as a result of subduction of a fossil spreading centre. We suggest that the thermal anomalies described in this paper are related to the northward migration of a subducting tear fault or slab window.

4.3. Exhumation through the ductile/brittle transition and subsequent rifting

Subsequent to this thermal anomaly, an exhumation and cooling from ~320 °C to 200 °C took place. ZFT ages are younger in the north when compared with the south along the Sundaland margin. Evidently, in all cases, ZFT ages are younger than the metamorphic age and the post kinematic intrusion. However, two dates from the south of the Gaoligong Shear Zone appear 10 Ma older than the extrapolation of the linear trend of the metamorphic event (Fig. 9).

The rifting in western Sundaland also follows a northward trend (Morley, 2016 and references therein). An exception is the central Burma Basin that formed in a fore-arc setting (Hall and Morley, 2004; Licht et al., 2013). Our observations show that AFT data follow a similar trend (Fig. 9). This second stage of exhumation could be closely linked to the rifting events as their age window overlaps that of the early sedimentary basin-infilling.

4.4. A northward migration of the chain of events

The Stong complex was affected by a strong deformation around 80 Ma associated with a thermal anomaly. This deformation took place within the amphibolite metamorphic facies and was followed by the intrusion of a non-deformed Noring pluton at ~75 Ma (U—Pb age, Ng et al., 2015a,b). Therefore, the latter is a stitching pluton, which is the source of numerous leucogranite dykes splaying into the surrounding metamorphics. An exhumation and cooling of the dome through ~320–200 °C was documented by ZFT ages of 72 Ma to 55 Ma, near the base of the brittle crust. The exhumation was facilitated by a low angle detachment located on the southern flank of the dome (François et al., 2017). The final unroofing stage is recorded by cooling through ~120–60 °C between 45 Ma and 30 Ma. No sedimentary basins are obvious around the Stong complex, probably due to significant subsequent erosion.

The Khanom dome was affected by ductile deformation within the amphibolite facies at ~72 Ma followed by the intrusion of a post-kinematic granite at 68 Ma (Kawakami et al., 2014). It was subsequently exhumed during Eocene - Oligocene times with an overall cooling rate of 23 °C/Ma. The thermal model appears to follow similar cooling trends as compared to the Stong Complex (François et al., 2017). ZFT ages centred at 33 Ma testify of a strong Late Eocene to Oligocene exhumation. The initial fast cooling rates (30 °C / Ma from 36 to 32 Ma) are interpreted to be the result of rapid exhumation through high angle normal faults. The structures accommodating the Eocene to Oligocene exhumation are large E–W normal faults with an apparent top-south offset (Fig. 5). They are in agreement with the final N—S stretching of the upper crust accompanying a likely deeper ductile elongation of an intermediate or lower crust, which had been previously thickened during the E-W compression in the Late Cretaceous (Sautter et al., 2017; Morley, 2012). Several studies have indeed revealed the existence of E–W striking valleys beneath the main *syn*-rift sequences in different basins of Sundaland (e.g., Mansor et al., 2014; Pubellier and Morley, 2014; Tjia, 1998). The rifting took place in the nearby Nakhon Basin from the Early Oligocene to the Early Miocene (Sautter et al., 2017;

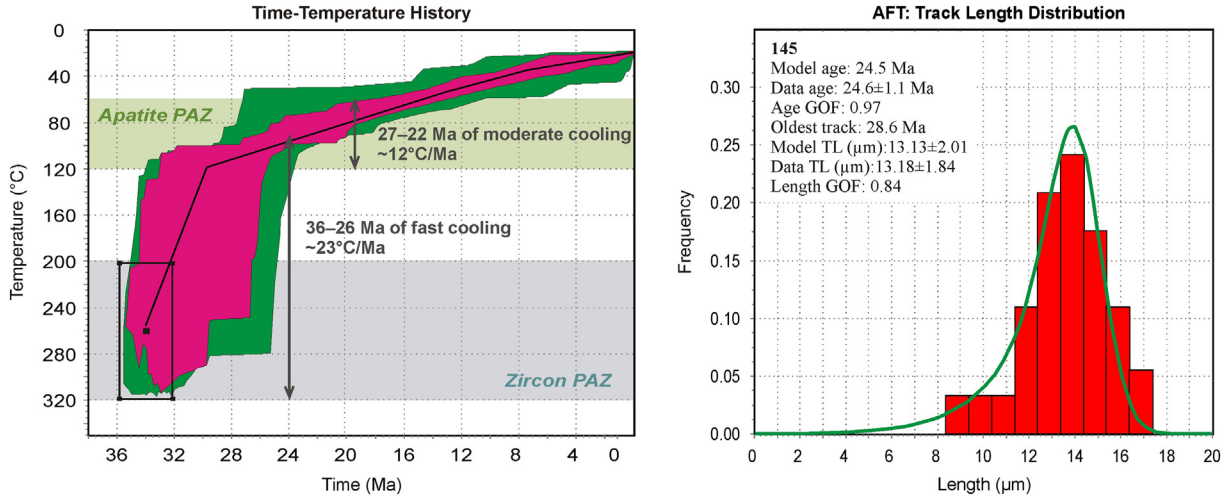

Fig. 8. Thermal modelling of AFT data (sample 145) obtained by HeFTy program (Ketcham, 2005). Results are displayed in time-temperature diagram (left diagram). Magenta envelope – good fit; green envelope – acceptable fit; black line – best fit; black box – fixed constraint defined according to independent geological data (ZFT age). Right diagram – frequency distribution of measured confined track length data overlain by a calculated probability density function (best fit). Model age, Data age – model and data calculated age. Age GOF, Length GOF – goodness of fit (statistical comparison of the measured input data and modelled output data, where a "good" result corresponds to value 0.5 or higher, "the best" result corresponds to value 1). Note that modelled t-T paths are valid only inside 120–60 °C (Apatite PAZ–partial annealing zone). Outside this temperature range must not necessarily represent the real thermal trajectory of a sample unless constrained by other data. Oldest track: the age of the oldest fission track that has not fully annealed. Model TL, Data TL – mean lengths of the model and data, and the standard deviations of length distributions. (For interpretation of the references to colour in this figure legend, the reader is referred to the web version of this article.)

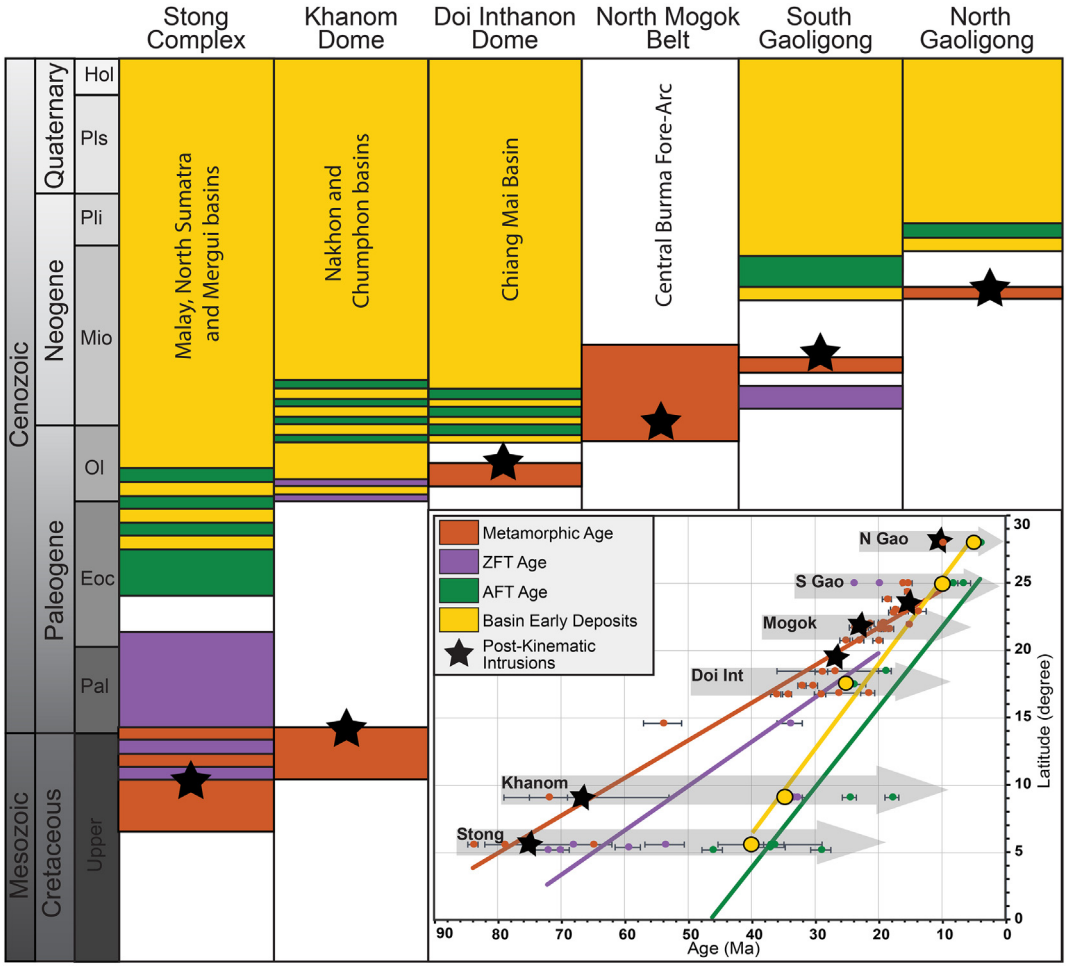

Fig. 9. Chrono-diagram showing the evolution of metamorphic events, post-kinematic intrusions ages, fission tracks ages and rift basin deposits with time. Inset represents an age-versus-latitude diagram compiling published geochronological data (available in Table 3) in metamorphism, fission tracks and average age of early Cenozoicsyn-rift sediments as well as unpublished fission tracks data. Mean linear trend are represented in the data sets respective colours.

Table 3
Synthesis of published geochronological data in metamorphism, fission tracks and average age of early Cenozoicsyn-rift sediments.

Metamorphic dome	Latitude	Magmatic Age	Metamorphic Age	ZFT	AFT	Basin Early Deposits
Stong						
Stong Berangkat	5.2	231.8 ± 1.7 [1]		70.3 ± 1.6 [8]	46.2 ± 1.6 [8]	
Stong Kenerong	5.4			59.5 ± 2 [8]	37.2 ± 2.5 [8]	
Stong Kenerong	5.2			72.2 ± 2.5 [8]	29.1 ± 1.6 [8]	
Stong Kenerong	5.6	220.4 ± 3.9 [1]	83.9 ± 0.8 [1]	68.2 ± 6.2 [8]	37.1 ± 8.2 [8]	40 (Malay)
Stong Kenerong	5.6		79 ± 3 [2]			40 (N Sumatra/Mergui)
Stong Kenerong	5.6		65 [3]			
Stong Noring	5.6	75.7 ± 0.6 [1]		53.7 ± 3.1 [8]	36.5 ± 1.6 [8]	
Stong Noring	5.6	69 ± 1 [2]				
Stong Noring	5.6	70 ± 2 [2]				
Stong Jeli	5.7	65 ± 2 [2]				
Stong Jeli	5.7	76 ± 2 [2]				
Stong Kemahang	5.8	226.7 ± 2.2 [1]	107 ± 3 [3]	90.3 ± 2.2 [8]	38.7 ± 1.4 [8]	
Khanom						
Khao Pret Granite	9.1	67.5 ± 1.3 [4a]		32.9 ± 1.6 [9]	17.9 ± 1.1 [9]	35 (Nakhon/Chumphon)
Khao Dat Fa granite	9.1	477 ± 7 [4a]		33.5 ± 1.5 [9]	24.6 ± 1.1 [9]	
Khao Dat Fa granite	9.1	205 ± 25 [4b]				
Haad Nai Phlao gneiss	9.1		72 ± 13 [4b]			
Laem Thong Yang gneiss	9.1	263 ± 36 [4b]				
Laem Thong Yang gneiss	9.1		66 ± 9 [4b]			
Doi Inthanon						
Mae Klang Waterfall gneiss	18.4	210 [5]	29 ± 3 [5]			
Mae Ya Waterfall gneiss	18.5	217 ± 8 [5]	27 ± 1 [5]			
Dyke into gneiss	17.5				24 ± 2 [10]	25 (Chiang Mai)
Gneiss	18.5				19 ± 1 [10]	
Thabsila						
Gneiss	14.6		54 ± 3 [6a]	34 ± 2 [6b]		28 (Suphan Buri)
Mogok						
Mogok South Thaton	16.85		26.4 ± 1.1 [7a]			
Mogok South Thaton	16.85		21.7 ± 0.7 [7a]			
Mogok South Thaton	17.43		25.2 ± 0.8 [7a]			
Mogok Central Meiktila	20.73		20.1 ± 0.8 [7a]			
Mogok Central Meiktila	20.75		25.3 ± 0.9 [7a]			
Mogok Central Meiktila	20.75		23.2 ± 0.8 [7a]			
Mogok N Shan scarp	21.6		18.4 ± 0.4 [7b]			
Mogok N Shan scarp	21.7		22.8 ± 0.4 [7a]			
Mogok N Shan scarp	21.7		23 ± 0.5 [7b]			
Mogok N Shan scarp	21.7		22.4 ± 0.8 [7b]			
Mogok N Shan scarp	21.7		22.4 ± 0.8 [7a]			
Mogok N Shan scarp	22		21.5 ± 0.6 [7c]			
Mogok N Shan scarp	22.06		19.4 ± 0.3 [7a]			
Mogok Sagaing Fault	21.93		19.8 ± 0.3 [7c]			
Mogok Sagaing Fault	21.93		15.3 ± 0.3 [7b]			
Mogok NE Shan Plateau	24.36		15.6 ± 0.7 [7a]			
Mogok NE Shan Plateau	23.8		18.7 ± 0.6 [7a]			
Mogok NE Shan Plateau	22.81		17.8 ± 0.9 [7a]			
Mogok NE Shan Plateau	22.91		16.6 ± 0.6 [7a]			
Mogok NE Shan Plateau	23.03		17.5 ± 1.4 [7a]			
Mogok NE Shan Plateau	22.91		13.9 ± 1.1 [7a]			
Mogok Northern Shan scarp	21.7		22.3 ± 0.7 [7d]			
Mogok Northern Shan scarp	21.7		23.9 ± 0.6 [7d]			
Mogok Northern Shan scarp	21.6		19.1 ± 0.5 [7e]			
Mogok Northern Shan scarp	21.6		20 ± 0.5 [7e]			
Mogok South Thaton	17.4		32.2 ± 0.9 [7d]			
Mogok South Thaton	17.4		30.5 ± 0.9 [7f]			
Mogok South Thaton	16.76		29.2 ± 0.7 [7d]			
Mogok South Thaton	16.76		34.4 ± 0.8 [7f]			
Mogok South Thaton	16.76		36.2 ± 0.8 [7f]			
Gaoligong						
South	25		15.5 ± 0.1 [7a]	20 [11]	6.8 ± 1.3 [11]	10
South	25		16.3 ± 0.1 [7a]	24 [11]	8.4 ± 0.9 [11]	
North	28		10 ± 0.1 [7a]		4 [12]	5

Note: Ages are provided by: [1] Ng et al. (2015): U–Pb zircon; [2] Bignell and Snelling (1977): K–Ar Whole Rock; [3] Darbyshire (1988): K–Ar Muscovite; [4] Kawakami et al. (2014): [4a] U–Pb Zircon; [4b] CHIME Monazite core; [5] Gardiner et al. (2016): U–(Th)–Pb zircon; [6] Nantasin et al. (2012): [6a] U–Pb Zircon [6b] Rb–Sr Biotite; [7] Bertrand et al. (2001): [7a] Ar/Ar Biotite [7b] Ar/Ar Muscovite [7c] Ar/Ar Phlogopite [7d] K/Ar Biotite [7e] K/Ar Muscovite [7f] K/Ar Feldspar; [8] François et al. (2017); [9] This Study;[10] Upton et al. (1997); [11] Wang et al. (2008); [12] Lei et al. (2006).

Morley, 2016) and the opening of its southern continuation (Songkhla Basin) started from the Late Eocene (Phoosongsee and Morley, 2018). The occurrence of Low Angle Normal Faults in the Thai Basins has been evidenced by several authors and is generally associated with large scale extensional exhumation accommodated by crustal detachments (Sautter et al., 2017; Morley, 2009). Exhumation to shallower depth occurred from the Late Oligocene to the Early Miocene as illustrated by AFT ages of ~25 Ma and 18 Ma and probably reflect minor brittle normal faulting without enhanced exhumation. In summary, the evolution of the Khanom and adjacent area follows a general pattern observed in many extensional domes worldwide, which show rapid exhumation of footwalls associated with the formation of brittle faults and sedimentary basins in their late evolutionary stages.

The Doi Inthanon and Doi Suthep are two metamorphic core complexes in northern Thailand ductilely deformed in the Oligocene followed by post-kinematic intrusions at 27 Ma (Dunning et al., 1995). The Chiang Mai Basin formed by the end of the Oligocene and available AFT ages indicate an exhumation and cooling to upper crustal levels between ~24 Ma and 18 Ma (Mankhemthong et al., 2018; Morley, 2009; Morley et al., 2011; Upton, 1999). Upton et al. (1997), conducted a thermal modelling for one sample with sufficient track lengths of the Doi Inthanon complex, and estimated cooling rates between 8.5 °C / Ma and 25 °C / Ma corresponding to a denudation of 550–3500 m/Ma which is in accordance with our cooling rates through the APAZ in Khanom. The author interprets this event as a rapid cooling through the Apatite PAZ. The major shear zones of the region underwent transpression followed by an extensional reactivation (Morley, 2004), thus supporting the observation of the northward migration of a unique phenomenon.

The domes further north, are characterized by similar physical and structural properties, but the chronology of their exhumation appears more complex and their evolutionis also faster.

The Mogok Metamorphics were ductilely deformed between ~25 Ma and 15 Ma at latitudes 22–25°N (Mitchell et al., 2012; Searle et al., 2007). The southern domes have been intruded by a less deformed leucogranite dyke around ~24 Ma (Searle et al., 2007). However, no fission track data is available in this region.

Finally, in the Gaoligong region, a ductile shear occurred from the Oligocene to the Late Miocene (Wang et al., 2008). Less deformed leucogranite intrusions are dated at 10–11 Ma. Pliocene sedimentary basins developed nearby, synchronous to a late exhumation recorded through AFT data clustering around ~4 Ma.

4.5. Ductile stretching of intermediate to lower crust accompanied by granitic intrusions: an interplate shear zone or a paleo-crustal flow?

We propose a simplified conceptual 3D model that accounts for a lower crustal ductile shear rooted at the base of the upper plate (Sundaland continental crust) as the Indian Plate was migrating northward from the Paleogene to the Present (Fig. 10). It reflects the relative motion between the two plates. The northward migration of the buoyant Indian Plate together with its northern passive margin is inferred to have scrapped off the base of the Eurasian crust during underplating due to an enhanced coupling between the two plates. The regional character and the pervasive mechanics of this process (Fig. 9), is justified by consistent observations from Malaysia in the south to northeastern Myanmar in the north, which represent a narrow zone of < 500 km from the present-day plate margin. The metamorphic event associated with the intense shearing, formed in response to deformation at the initial contact between the subducting Greater India and Sundaland after the subduction of the thinner Neo-Tethys oceanic crust, which generated significant extension and exhumation. Therefore, we directly infer underplating of a thinned continental crust beneath a thick continental crust. It is assumed that, similarly to the models on the hard indentation of the Indian Plate into Eurasia, fragments of crustal blocks may have been extruded southward before the start of the channel flow process, more precisely before the ductile response to the high crustal thickness anomaly. Following this interpretation, between 40 Ma and 30 Ma, the eastern side of Malay Peninsula, sandwiched between the Khlong Marui Fault and the Mae Ping Fault (Figs. 1 and 2) would have been extruded southward through a sinistral motion of the Mae Ping Fault and a dextral motion of the Ranong and Khlong Marui faults. Whereas, after 30 Ma, the Mergui Terrane (west of the Ranong Fault) would have been extruded southwestward with a sinistral motion along the Ranong Fault and a dextral motion along the TPF and MPF. These motions are believed to be a form of dislocations rather than large long-lasting rigid block migrations. In order to balance the resulting mass anomaly, a collapse towards the south of the Sunda crust would occur, possibly together with a southward escape of lower crustal ductile material invoked in a manner similar to that of the present-day East Himalayan Syntaxis (Clark and Royden, 2000; Maurin and Rangin, 2009; Rey et al., 2001; Searle and Szulc, 2005). This ductile flow of material may accompany the relative motion between the two plates and account for the variation of crustal thicknesses. The trace of this event would result in significant crustal thickness variations, as observed in Peninsular Malaysia (Abdul Latiff and Khalil, 2018). The excess of thicker crust induced thermal anomalies that resulted in post kinematic intrusions, crosscutting metamorphic foliations and shearing zones. This was followed by an exhumation event that can be associated with the subduction of the Indian Plate and continent-ocean transition, characterized by tilted blocks inherited from the rifting from Gondwana. The underplating of this paleo-topographic feature is inferred to have generated a stronger coupling between the two plates with an “up –and-down” phenomena representing the short lifespan over which the topography was uplifted and supported (Spikings and Simpson, 2014). The paleo-topographic feature would have, firstly, created an uplift event when the ridge entered the subduction, followed by a gravitational collapse at the receding side, as it moved away towards the north. The resulting effects are seen along Peninsular Malaysia with large E-W normal faults showing an apparent top-to-south offset (Fig. 5). Early pre-rift sediments have been reported in most of the western Sundaland Cenozoic basins, which do not follow the subsequent rifting geometries (Bertrand et al., 2001; Mansor et al., 2014; Williams et al., 1995). Indeed, these early deposits are often oriented along E-W depressions; whereas, the bounding faults of rift basins dominantly strike N-S. Finally, past the migration of India towards the north and its indentation into the Eurasian Plate, a global relaxation is illustrated by the incipient rifting of the edge of Sundaland and late exhumation stage of the crustal horst highlighted through AFT data.

We propose that the younging of the metamorphism, exhumation ages as well as the rifting in the Tertiary represent a paleo-position of the East Himalayan Syntaxis, migrating northward with time (Figs. 1b, c and d). The presence of important N-S topographic gradients in the basement rocks of the Peninsula support this hypothesis (e.g., Thai Batholith and Malay Batholith shown in Fig. 2).

The ductile crust is exposed along exhumed high-temperature metamorphic domes that are not located randomly. These complexes protrude within or on the side of the large Mesozoic Yenshanian magmatic arc. A recent study showed that the quartz concentration in the crust is critical for the initiation of a lower crustal flow(Lowry and Perez-Gussinye, 2011). These authors demonstrated that the regions more prone to flow are those with high quartz concentration, and therefore, a crust, severely intruded by granitic plutons, is a good candidate. Since information on the overall crustal chemistry in SE Asia is scarce, field studies in western Sundaland reveal that the Malay Peninsula is cored by numerous massive plutons crosscut by massive quartz dykes (e.g., Main Range Province). Although, on either side, the thinner crust is marked by prominent mafic intrusions (e.g., dykes and basaltic flows around the Gulf of Thailand and mafic intrusions in the Andaman Sea after Morley (2017)). Throughout, a Vp/Vs and Poisson ratio study by Noisagool et al. (2014), revealed a mafic lower crust

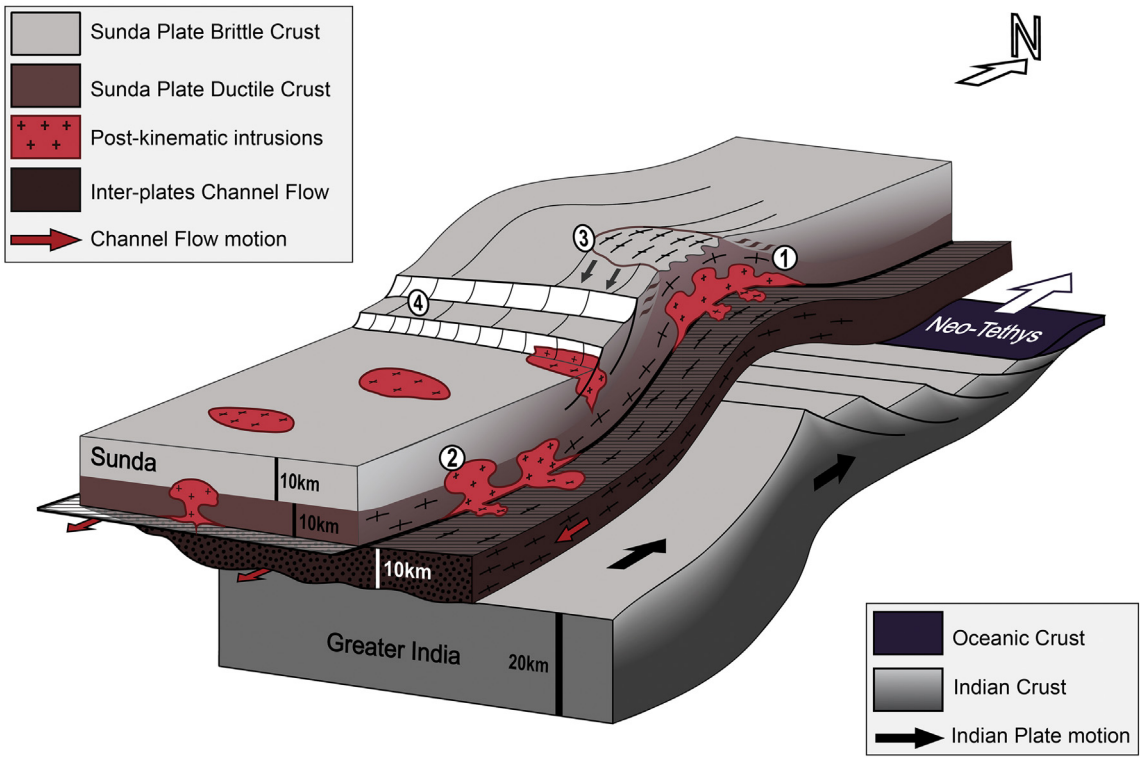

Fig. 10. 3D bloc diagram of the proposed channel flow model. The upper Eurasian Plate (Sunda) is fixed whereas the Indian lithosphere is migrating towards the north (see Fig. 1c for location). The kink between the Indian stretched margin and thick continental crust dynamically scrapped off basal Eurasian lithosphere while underplating, and a supposed channel flow propagated towards the south. The numbering highlights the chronology of the successive processes.

beneath the Khorat Plateau. Southward, granulite xenoliths have been found in Cenozoic basalts on the shore of the Thai Gulf (Promprated and Taylor, 2003); whereas, on the western super-stretched side of the Peninsula, several studies reveal a dense lower crust beneath the Andaman Basins (Curray, 2005; Morley, 2015). Therefore, western Sundaland is structured in two distinct domains; 1) a quartz-rich peninsula backbone with deep metamorphic core complexes exhumed on its edges and bordered by, 2) two mafic lower crustal domains subjected to intense thinning during the rifting.

Fig. 9 shows that in the northern part of the region, the successive deformation events appear in a similar order but faster than that in the south. If not due to a better precision in the compiled ages (Table 3), this can indicate a thinner upper plate, possibly due to tectonic erosion that resulted in a sharp topography contrast when a thicker Indian crust subducted beneath northern Sundaland (Gaoligong, Mogok and present-day syntaxis). This would create a difference of wavelength of the crustal asperity passing beneath Sunda: a large bulge in the south, which would need longer time to re-equilibrate and a narrower kink in the north with fast collapse. The crustal topography could as well be the step between the thick Indian lithosphere and a thinner greater Indian lithosphere, which would be currently located under the present trace of the Sagaing Fault. As a result, the Malay Peninsula would have experienced a moderate doming and slow exhumation following the subduction of Greater India lithosphere; whereas, the Mogok and Gaoligong would have experienced the subduction of the thick Indian lithosphere after the Miocene.

5. Conclusion

We observe, along a N-S transect from the southern Peninsular Malaysia to the East Himalayan Syntaxis, an overall correlation between Late Cretaceous to Late Miocene metamorphic events and subsequent exhumation and basin development.

We propose that during the N-S migration of the Indian Plate, the necking between its stretched margin and thick continental crust dynamically scrapped off the basal Eurasian lithosphere while underplating. This process may depict the first stage of crustal thickening, as observed further north, in front of the location of “hard” indentation of India and appears responsible for thermal instabilities associated with leucogranite intrusions. The resulting deformation could be imprinted in the ductile crust that crops out at several localities owing to late extension. The extension is expressed in a ductile manner in the early stages and later becomes brittle, resulting in the widespread development of basins in the upper levels of the upper plate crust.

We infer that this phenomenon migrated to the north as the Indian Plate was indenting into the Eurasian Plate. Therefore, information that is now hidden in the Himalaya appear to be preserved laterally on the western margin of Sundaland. The clear common succession of events in each region allows for extrapolation of the correlation between metamorphic ages, exhumation ages, and early rifted basins, and would record the migration of the Indian Plate towards the north, relative to the Eurasia and Sunda plates. The suggested concept for the mechanism can be improved with further geological observations along transects that include areas where deformation occurs in the eastern Himalaya.

Acknowledgements

The authors would like to thank an anonymous reviewer and Prof Christopher Morley for their suggestions and critical and constructive reviews that greatly helped improve the scientific quality of the manuscript. The authors thank the editor Dr. Shuhab Khan for a thorough editorial work. This work would not have been possible without funding from Total E&P, the Ecole Normale Supérieure in Paris, and a cooperation with the Universiti Teknologi Petronas. Processing of the samples was ensured by the Comenius University in Bratislava, Slovakia, and the University of Amsterdam in the Netherlands. One of the authors (MP) was supported by the CNRS (France) and hosted by the Ecole Normale Supérieure during the compilation of the data.

References

Abdul Latiff, A.H., Khalil, A.E., 2018. Crustal thickness and velocity structure of Malay Peninsula inferred from joint inversion of receiver functions and surface waves dispersion. J. Asian Earth Sci. 0–1. https://doi.org/10.1016/j.jseaes.2018.08.011.

Ali, J.R., Aitchison, J.C., 2005. Greater India. Earth Sci. Rev. 72, 169–188. https://doi.org/10.1016/j.earscirev.2005.07.005.

Ali, J.R., Aitchison, J.C., 2008. Gondwana to Asia: Plate tectonics, paleogeography and the biological connectivity of the Indian sub-continent from the Middle Jurassic through latest Eocene (166-35 Ma). Earth Sci. Rev. 88, 145–166. https://doi.org/10.1016/j.earscirev.2008.01.007.

Ali, M.A., Willingshofer, E., Matenco, L., Francois, T., Daanen, T.P., Ng, T.F., Taib, N.I., Shuib, M.K., 2016. Kinematics of post-orogenic extension and exhumation of the Taku Schist, NE Peninsular Malaysia. J. Asian Earth Sci. 127, 63–75. https://doi.org/10.1016/j.jseaes.2016.06.020.

Beckinsale, R.D., Suensilpong, S., Nakapadungrat, S., Walsh, J.N., 1979. Geochronology and geochemistry of granite magmatism in Thailand in relation to a plate tectonic model. J. Geol. Soc. Lond. 136, 529–540. https://doi.org/10.1144/gsjgs.136.5.0529.

Bertrand, G., Rangin, C., Maluski, H., Han, T.A., Thein, M., Myint, O., Maw, W., Lwin, S., 1999. Cenozoic metamorphism along the Shan scarp (Myanmar): Evidences for ductile shear along the Sagaing fault or the northward migration of the eastern Himalayan syntaxis? Geophys. Res. Lett. 26, 915–918. https://doi.org/10.1029/1999GL900136.

Bertrand, G., Rangin, C., Maluski, H., Bellon, H., Scientific Party, G.I.A.C., 2001. Diachronous cooling along the Mogok Metamorphic Belt (Shan scarp, Myanmar): the trace of the northward migration of the Indian syntaxis. J. Geophys. Res. 19, 649–659.

Bignell, J.D., Snelling, N.J., 1977. K-Ar ages on some basic igneous rocks from Peninsular Malaysia and Thailand. Geol. Soc. Malaysia Bull 8, 89–93 (December).

Blomme, K., 2013. Apatite Fission-Track Thermochronology and Petrographic Characterization of South Thailand Granitoids : Evolution of the Andaman Basin with Respect to the Eastern Indian Passive Margin.

Boettcher, S.S., Milliken, K.L., 2009. Mesozoic-cenozoic unroofing of the southern appalachian basin: apatite fission track evidence from middle pennsylvanian sandstones. J. Geol. 102, 655–668. https://doi.org/10.1086/629710.

Burtner, R., Nigrini, A., Donelick, R.A., 1994. Thermochronology of Lower Cretaceous source rocks in the Idaho-Wyoming thrust belt. Am. Assoc. Pet. Geol. Bull. 78, 1613–1636.

Charusiri, P., Clark, A.H., Farrar, E., Archibald, D., Charusiri, B., 1993. Granite belts in Thailand: evidence from the 40Ar/39Ar geochronological and geological syntheses. J. SE Asian Earth Sci. 8, 127–136. https://doi.org/10.1016/0743-9547(93)90014-G.

Clark, M.K., Royden, L.H., 2000. Topographic ooze:building the eastern margin of Tibet by lower crustal flow. Geology 28, 703–706. https://doi.org/10.1130/0091-7613(2000)28<703:Tobtem>2.0.Co;2.

Cobbing, E.J., Pitfield, P.E.J., Darbyshire, D., Mallick, D.I.J., Pitfield, P.E.J., Teoh, L.H., 1986. The granites of the Southeast Asian Tin Belt. J. Geol. Soc. Lond. 143, 537–550. https://doi.org/10.1144/gsjgs.143.3.0537.

Copley, A., Avouac, J.P., Royer, J.Y., 2010. India-Asia collision and the Cenozoic slowdown of the Indian plate: Implications for the forces driving plate motions. J. Geophys. Res. Solid Earth 115, 1–14. https://doi.org/10.1029/2009JB006634.

Cottam, M.A., Hall, R., Ghani, A.A., 2013. Late cretaceous and cenozoic tectonics of the Malay Peninsula constrained by thermochronology. J. Asian Earth Sci. 76, 241–257. https://doi.org/10.1016/j.jseaes.2013.04.029.

Curray, J.R., 2005. Tectonics and history of the Andaman Sea region. J. Asian Earth Sci. 25, 187–232. https://doi.org/10.1016/j.jseaes.2004.09.001.

Dunning, G.R., Macdonald, A.S., Barr, S.M., 1995. Zircon and monazite UPb dating of the Doi Inthanon core complex, northern Thailand: implications for extension within the Indosinian Orogen. Tectonophysics 251, 197–213. https://doi.org/10.1016/0040-1951(95)00037-2.

Eroğlu, S., Siebel, W., Danišík, M., Pfänder, J.A., Chen, F., 2013. Multi-system geochronological and isotopic constraints on age and evolution of the Gaoligongshan metamorphic belt and shear zone system in western Yunnan, China. J. Asian Earth Sci. 73, 218–239. https://doi.org/10.1016/j.jseaes.2013.03.031.

Fabian, T., Whittaker, J., 2010. Mapping Tertiary Mid-Ocean Ridge Subduction and Slab Window Formation beneath Sundaland Using Seismic Tomography. Aseg, pp. 1–4.

François, T., Ali, M.A., Willingshofer, E., Ng, T.F., Taib, N.I., Shuib, M.K., 2017. Late Cretaceous extension and exhumation of the Stong complex and Taku Schist, NE Peninsular Malaysia. J. Asian Earth Sci. 143, 296–314.

Fyhn, M.B.W., Green, P.F., Bergman, S.C., Van Itterbeeck, J., Tri, T.V., Dien, P.T., Abatzis, I., Thomsen, T.B., Chea, S., Pedersen, S.A.S., Mai, L.C., Tuan, H.A., Nielsen, L.H., 2016. Cenozoic deformation and exhumation of the Kampot Fold Belt and implications for South Indochina tectonics. J. Geophys. Res. Solid Earth 121, 5278–5307. https://doi.org/10.1002/2016JB012847.

Galbraith, R.F., 1981. On statistical models for fission track counts. Math. Geol. 13, 471–478.

Gardiner, N.J., Searle, M.P., Robb, L.J., Morley, C.K., 2015. Neo-Tethyan magmatism and metallogeny in Myanmar - an Andean analogue? J. Asian Earth Sci. 106, 197–215. https://doi.org/10.1016/j.jseaes.2015.03.015.

Gardiner, N.J., Roberts, N.M.W., Morley, C.K., Searle, M.P., Whitehouse, M.J., 2016. Did Oligocene crustal thickening precede basin development in northern Thailand? A geochronological reassessment of Doi Inthanon and Doi Suthep. Lithos 240–243, 69–83. https://doi.org/10.1016/j.lithos.2015.10.015.

Ghani, A.A., 2000. Mantled feldspar from the Noring granite, Peninsular Malaysia: petrography, chemistry and petrogenesis. Bull. Geol. Soc. Malaysia 44, 109–115.

Ghani, A.A., 2009. Plutonism. Geol. Penins. Malaysia 2232.

Ghani, A.A., Searle, M., Robb, L., Chung, S.L., 2013. Transitional I S type characteristic in the Main Range Granite, Peninsular Malaysia. J. Asian Earth Sci. 76, 225–240. https://doi.org/10.1016/j.jseaes.2013.05.013.

Gibbons, A.D., Whittaker, J.M., Muller, R.D., 2013. The breakup of East Gondwana: Assimilating constraints from cretaceous ocean basins around India into a best-fit tectonic model. J. Geophys. Res. Solid Earth 118, 808–822. https://doi.org/10.1002/jgrb.50079.

Gibbons, A.D., Zahirovic, S., Müller, R.D., Whittaker, J.M., Yatheesh, V., 2015. A tectonic model reconciling evidence for the collisions between India, Eurasia and intra-oceanic arcs of the central-eastern Tethys. Gondwana Res. 28, 451–492. https://doi.org/10.1016/j.gr.2015.01.001.

Hall, R., 2002. Cenozoic geological and plate tectonic evolution of SE Asia and the SW Pacific: Computer-based reconstructions, model and animations. J. Asian Earth Sci. 20, 353–431. https://doi.org/10.1016/S1367-9120(01)00069-4.

Hall, R., Morley, C.K., 2004. Sundaland Basins. Cont. Interact. Within East Asian Marg. Seas. pp. 55–85. https://doi.org/10.1029/149gm04.

Hassan, W.F.W., Hamzah, M.S., 1998. Rare earth element patterns in some granitic rocks of Peninsular Malaysia. In: GEOSEA '98, Ninth Reg. Congr. Geol. Miner. Energy Resour. South East Asia, pp. 196–197.

Heward, A.P., Chuenbunchom, S., Makel, G., Marsland, D., Spring, L., 2000. Nang Nuan oil field, B6/27, Gulf of Thailand: karst reservoirs of meteoric or deep-burial origin? Pet. Geosci. 6, 15–27. https://doi.org/10.1144/petgeo.6.1.15.

Huang, X., Xu, Z., Li, H., Cai, Z., 2015. Tectonic amalgamation of the Gaoligong shear zone and Lancangjiang shear zone, southeast of Eastern Himalayan Syntaxis. J. Asian Earth Sci. 106, 64–78. https://doi.org/10.1016/j.jseaes.2014.12.018.

Hutchison, C.S., 1977. Granite Emplacement and Tectonic Subdivision of Peninsular Malaysia. Geol. Soc.

Hutchison, C.S., 2013. Geology of Tin Deposits. J. Chem. Inf. Model. https://doi.org/10.1017/CBO9781107415324.004.

Ismail, A., Ghani, A.A., Rozi Umor, M., Shaarani, N.A., 2003. Field relation, petrochemistry and classification of the volcanic rocks from the eastern part of Tioman Island, Pahang. Geol. Soc. Malaysia, Bull. 46, 415–419.

Jacob, J., Dyment, J., Yatheesh, V., 2014. Revisiting the structure, age, and evolution of the Wharton Basin to better understand subduction under Indonesia. J. Geophys. Res. Solid Earth 119, 169–190. https://doi.org/10.1002/2013JB010285.

Kanjanapayont, P., Klötzli, U., Thöni, M., Grasemann, B., Edwards, M.A., 2012. Rb–Sr, Sm–Nd, and U–Pb geochronology of the rocks within the Khlong Marui shear zone, southern Thailand. J. Asian Earth Sci. 56, 263–275. https://doi.org/10.1016/j.jseaes.2012.05.029.

Kanjanapayont, P., Kieduppatum, P., Klötzli, U., Klötzli, E., Charusiri, P., 2013. Deformation history and U-Pb zircon geochronology of the high grade metamorphic rocks within the klaeng fault zone, eastern Thailand. J. Asian Earth Sci. 77, 224–233. https://doi.org/10.1016/j.jseaes.2013.08.027.

Kawakami, T., Nakano, N., Higashino, F., Hokada, T., Osanai, Y., Yuhara, M., Charusiri, P., Kamikubo, H., Yonemura, K., Hirata, T., 2014. U-Pb zircon and CHIME monazite dating of granitoids and high-grade metamorphic rocks from the Eastern and Peninsular Thailand - a new report of early Paleozoic granite. Lithos 200–201, 64–79. https://doi.org/10.1016/j.lithos.2014.04.012.

Ketcham, R.A., 2005. Forward and Inverse Modeling of Low-Temperature Thermochronometry Data. 58. pp. 275–314. https://doi.org/10.2138/rmg.2005.58.11.

Ketcham, R.A., Donelick, R.A., Carlson, W.D., 1999. Variability of apatite fission-track annealing kinetics; III. Extrapolation to geologic time scales. Am. Mineral. 84, 1235–1255.

Ketcham, R.A., Carter, A., Donelick, R.A., Barbarand, J., Hurford, A.J., 2007. Improved measurement of fission-track annealing in apatite using c-axis projection. Am. Mineral. 92, 789–798.

Klootwijk, C.T., Gee, J.S., Peirce, J.W., Smith, G.M., McFadden, P.L., 1992. An early India-Asia contact: paleomagnetic constraints from Ninetyeast Ridge, ODP Leg 121. Geology 20, 395–398. https://doi.org/10.1130/0091-7613(1992)020<0395:AEIACP>2.3.CO;2.

Kosuwan, S., 1996. Geology of the Khanom Gneissic Complexes, Amphoe Khanom, Changwat Nakhon Si Thammarat. Chulalongkorn University, Bangkok.

Krahenbuhl, R., 1991. Magmatism, tin mineralization and tectonics of the Main Range, Malaysian Peninsula: Consequences for the plate tectonic model of Southeast Asia based on Rb-Sr, K-Ar and fission track data. Geo. Soc. Malaysia, Bull. 29, 1–100.

Kwan, T.S., Krähenbühl, R., Jager, E., Krahenbuhl, R., Krähenbühl, R., Jager, E., 1992. Rb-Sr, K-Ar and fission track ages for granites from Penang Island, West Malaysia: an interpretation model for Rb-Sr whole-rock and for actual and experimental mica data. Contrib. Mineral. Petrol. 111, 527–542. https://doi.org/10.1007/BF00320907.

Lacassin, R., Maluski, H., Leloup, P.H., Tapponnier, P., Hinthong, C., Siribhakdi, K., Chuaviroj, S., Charoenravat, A., 1997. Tertiary diachronic extrusion and deformation of western Indochina: Structural and 40Ar/39Ar evidence from NW Thailand. J. Geophys. Res. 102, 10013–10037.

Licht, A., Reisberg, L., Fontaine, C., Soe, A.N., Jaeger, J., 2013. A palaeo Tibet – Myanmar connection? In: Reconstructing the Late Eocene Drainage System of Central Myanmar Using a Multi-Proxy Approach. 170. pp. 929–939.

Lowry, A.R., Perez-Gussinye, M., 2011. The role of crustal quartz in controlling Cordilleran deformation. Nature 471, 353–357. https://doi.org/10.1038/nature09912.

MacDonald, A.S., Barr, S.M., Dunning, G.R., Yaowanoiyothin, W., 1993. The Doi Inthanon metamorphic core complex in NW Thailand: age and tectonic significance. J. SE Asian Earth Sci. 8, 117–125. https://doi.org/10.1016/0743-9547(93)90013-F.

Macdonald, A.S., Barr, S.M., Miller, B.V., Reynolds, P.H., Rhodes, B.P., Yokart, B., 2010. P-T-t constraints on the development of the Doi Inthanon metamorphic core complex domain and implications for the evolution of the western gneiss belt, northern

Thailand. J. Asian Earth Sci. 37, 82–104. https://doi.org/10.1016/j.jseaes.2009.07.010.
Madon, M.B., Mansor, M.Y., 1999. The Petroleum Geology and Resources of Malaysia.
Mankhemthong, N., Morley, C.K., Takaew, P., Rhodes, B.P., 2018. Structure and evolution of the Ban Pong Basin, Chiang Mai Province, Thailand. J. Asian Earth Sci. 0–1. https://doi.org/10.1016/j.jseaes.2018.09.010.
Mansor, M.Y., Rahman, A.H.A., Menier, D., Pubellier, M., 2014. Structural evolution of Malay Basin, its link to sunda block tectonics. Mar. Pet. Geol. 58, 736–748. https://doi.org/10.1016/j.marpetgeo.2014.05.003.
Maurin, T., Rangin, C., 2009. Structure and kinematics of the Indo-Burmese Wedge: recent and fast growth of the outer wedge. Tectonics 28. https://doi.org/10.1029/2008TC002276.
Mitchell, A., Chung, S.L., Oo, T., Lin, T.H., Hung, C.H., 2012. Zircon U-Pb ages in Myanmar: Magmatic-metamorphic events and the closure of a neo-Tethys Ocean? J. Asian Earth Sci. 56, 1–23. https://doi.org/10.1016/j.jseaes.2012.04.019.
Molnar, P., Tapponnier, P., 1977. The Collision between India and Eurasia. Sci. Am. https://doi.org/10.1038/scientificamerican0477-30.
Morley, C.K., 2004. Nested strike-slip duplexes, and other evidence for late Cretaceous–Palaeogene transpressional tectonics before and during India–Eurasia collision, in Thailand, Myanmar and Malaysia. J. Geol. Soc. Lond. 161, 799–812. https://doi.org/10.1144/0016-764903-124.
Morley, C.K., 2009. Geometry and evolution of low-angle normal faults (LANF) within a Cenozoic high-angle rift system, Thailand: Implications for sedimentology and the mechanisms of LANF development. Tectonics 28, 1–30. https://doi.org/10.1029/2007TC002202.
Morley, C.K., 2012. Late cretaceous-early palaeogene tectonic development of SE Asia. Earth Sci. Rev. 115, 37–75. https://doi.org/10.1016/j.earscirev.2012.08.002.
Morley, C.K., 2015. Cenozoic structural evolution of the Andaman Sea: evolution from an extensional to a sheared margin. Geol. Soc. Lond. Spec. Publ. 431 (1), 39–61. https://doi.org/10.1016/j.chb.2013.04.024.
Morley, C.K., 2016. The impact of multiple extension events, stress rotation and inherited fabrics on normal fault geometries and evolution in the Cenozoic rift basins of Thailand. GSL Spec 439. https://doi.org/10.1144/SP439.3.
Morley, C.K., 2017. Cenozoic rifting, passive margin development and strike-slip faulting in the Andaman Sea: a discussion of established v. new tectonic models. Myanmar Geol. Resour. Tectonics 47, 27–50. https://doi.org/10.1144/M47.4.
Morley, C.K., Racey, A., 2011. In: Ridd, M.F., Barber, A.J., Crow, M.J. (Eds.), Tertiary Stratigraphy. The Geology of Thailand.
Morley, C.K., Charusiri, P., Watkinson, I., 2011. Structural geology of Thailand during the Cenozoic. Geol. Thail. 273–334.
Müller, R.D., Gaina, C., Tikku, A., Mihut, D., Cande, S.C., Stock, J.M., 2000. Mesozoic/Cenozoic tectonic events around Australia. Geophys. Monogr. Ser. 121, 161–188.
Nantasin, P., Hauzenberger, C., Liu, X., Krenn, K., Dong, Y., Thöni, M., Wathanakul, P., 2012. Occurrence of the high grade Thabsila metamorphic complex within the low grade Three Pagodas shear zone, Kanchanaburi Province, western Thailand: Petrology and geochronology. J. Asian Earth Sci. 60, 68–87. https://doi.org/10.1016/j.jseaes.2012.07.025.
Ng, S.W.P., Chung, S.L., Robb, L.J., Searle, M.P., Ghani, A.A., Whitehouse, M.J., Oliver, G.J.H., Sone, M., Gardiner, N.J., Roselee, M.H., 2015a. Petrogenesis of Malaysian granitoids in the Southeast Asian tin belt: part 1. Geochemical and Sr-Nd isotopic characteristics. Bull. Geol. Soc. Am. 127, 1209–1237. https://doi.org/10.1130/B31213.1.
Ng, S.W.P., Whitehouse, M.J., Searle, M.P., Robb, L.J., Ghani, A.A., Chung, S.L., Oliver, G.J.H., Sone, M., Gardiner, N.J., Roselee, M.H., 2015b. Petrogenesis of Malaysian granitoids in the Southeast Asian tin belt: part 2. U-Pb zircon geochronology and tectonic model. Bull. Geol. Soc. Am. 127, 1238–1258. https://doi.org/10.1130/B31214.1.
Noisagool, S., Boonchaisuk, S., Pornsopin, P., Siripunvaraporn, W., 2014. Thailand's crustal properties from tele-seismic receiver function studies. Tectonophysics 632, 64–75. https://doi.org/10.1016/j.tecto.2014.06.014.
Patriat, P., Achache, J., 1984a. India–Eurasia collision chronology has implications for crustal shortening and driving mechanism of plates. Nature 311, 615–621. https://doi.org/10.1038/311615a0.
Patriat, P., Achache, J., 1984b. India-Eurasia collision chro- nology has implications for crustal shortening and driving mechanism of plates. Nature 311, 615–621.
Pesicek, J.D., Thurber, C.H., Widiyantoro, S., Engdahl, E.R., DeShon, H.R., 2008. Complex slab subduction beneath northern Sumatra. Geophys. Res. Lett. 35, 1–5. https://doi.org/10.1029/2008GL035262.
Phoosongsee, J., Morley, C.K., 2018. Evolution of a major extensional boundary fault system during multi-phase rifting in the Songkhla Basin, Gulf of Thailand. J. Asian Earth Sci. https://doi.org/10.1016/j.jseaes.2018.08.028.
Polachan, S., Racey, A., 1994. Stratigraphy of the Mergui Basin, Andaman Sea: Implications for Petroleum Exploration. J. Pet. Geol. 17, 373–406.
Portenga, E.W., Bierman, P.R., 2011. Understanding earth's eroding surface with 10Be. GSA Today 21, 4–10. https://doi.org/10.1130/G111A.1.
Promprated, P., Taylor, L.A., 2003. Petrochemistry of mafic granulite xenoliths from the chantaburi basaltic field: implications for the nature of the lower crust beneath Thailand. Int. Geol. Rev. 45, 383–406.
Pubellier, M., Morley, C.K., 2014. The basins of Sundaland (SE Asia): Evolution and boundary conditions. Mar. Pet. Geol. 58, 555–578. https://doi.org/10.1016/j.marpetgeo.2013.11.019.
Pubellier, M., Rangin, C., Le Pichon, X., Ego, F., Nguyen, H., Nielsen, C., Rabaute, A., Tsang Hin Sun, D., Bousquet, R., 2001. Deep Offshore Tectonics of South East Asia (DOTSEA); a Synthesis of Deep Marine Data in SouthEast Asia.
Putthapiban, P., 1992. The Cretaceous-Tertiary Granite Magmatism in the West Coast of Peninsular Thailand and the Mergui Archipelago of Myanmar/Burma. Thailand, D. of M.R. of (Ed.) In: National Conference on Geologic Resources of Thailand: Potential for Futur Development, pp. 75–88 Bangkok, Thailand.
Racey, A., Love, M.A., Duddy, I.R., Love, M.A., 1997. Apatite Fission Track Analysis of Mesozoic Red Beds from Northeastern Thailand and Western Laos. Int. Conf. Stratigr. Tecton. Evol. Southeast Asia South Pacific 1, 200–209.
Ramkumar, M., Menier, D., Mathew, M., Santosh, M., 2016. Geological, geophysical, and inherited tectonic imprints on the climate and contrasting coastal geomorphology of the Indian peninsula. Gondwana Res. 36, 52–80. https://doi.org/10.1016/j.gr.2016.04.008.
Ramkumar, M., Menier, D., Mathew, M., Santosh, M., Siddiqui, N.A., 2017. Early Cenozoic rapid flight enigma of the Indian subcontinent resolved: Roles of topographic top loading and subcrustal erosion. Geosci. Front. 8, 15–23. https://doi.org/10.1016/j.gsf.2016.05.004.
Replumaz, A., Tapponnier, P., 2003. Reconstruction of the deformed collision zone between India and Asia by backward motion of lithospheric blocks. J. Geophys. Res. 108, 24. https://doi.org/10.1029/2001JB000661.
Replumaz, A., Kárason, H., van der Hilst, R.D., Besse, J., Tapponnier, P., 2004. 4-D evolution of SE Asia's mantle from geological reconstructions and seismic tomography. Earth Planet. Sci. Lett. 221, 103–115. https://doi.org/10.1016/S0012-821X(04)00070-6.
Rey, P., Vanderhaeghe, O., Teyssier, C., 2001. Gravitational collapse of the continental crust: Definition, regimes and modes. Tectonophysics 342, 435–449. https://doi.org/10.1016/S0040-1951(01)00174-3.
Rhodes, B.P., Blum, J., Devine, T., 2000. Structural development of the Mid-Tertiary Doi Suthep Metamorphic complex and Western Chiang Mai Basin, Northern Thailand. J. Asian Earth Sci. 18, 97–108. https://doi.org/10.1016/S1367-9120(99)00019-X.
Sautter, B., Pubellier, M., 2015. Did the Malaysian Main Range record a weak hot mega Shear? Geophys. Res. Abstr. 17 (EGU2015-5167-1, 2015 17, 5167).
Sautter, B., Pubellier, M., Jousselin, P., Dattilo, P., Kerdraon, Y., Choong, C.M., Menier, D., 2017. Late Paleogene rifting along the Malay Peninsula thickened crust. Tectonophysics 710–711, 205–224. https://doi.org/10.1016/j.tecto.2016.11.035.
Schwartz, M.O., Rajah, S.S., Askury, A.K., Putthapiban, P., Djaswadi, S., 1995. The Southeast Asian tin belt. Earth Sci. Rev. 38, 95–293. https://doi.org/10.1016/0012-8252(95)00004-T.
Searle, M.P., Szulc, A.G., 2005. Channel flow and ductile extrusion of the high Himalayan slab-the Kangchenjunga-Darjeeling profile, Sikkim Himalaya. J. Asian Earth Sci. 25, 173–185. https://doi.org/10.1016/j.jseaes.2004.03.004.
Searle, M.P., Noble, S.R., Cottle, J.M., Waters, D.J., Mitchell, A.H.G., Hlaing, T., Horstwood, M.S.A., 2007. Tectonic evolution of the Mogok metamorphic belt, Burma (Myanmar) constrained by U-Th-Pb dating of metamorphic and magmatic rocks. Tectonics 26. https://doi.org/10.1029/2006TC002083.
Searle, M.P., Whitehouse, M.J., Robb, L.J., Hutchison, C.S., Sone, M., Ng, S.W.-P., Roselee, M.H., Chung, S.-L., Oliver, G.J.H., Ghani, a.a., Hutchison, C.S., Sone, M., Ng, S.W.-P., Roselee, M.H., Chung, S.-L., Oliver, G.J.H., 2012. Tectonic evolution of the Sibumasu-Indochina terrane collision zone in Thailand and Malaysia: constraints from new U-Pb zircon chronology of SE Asian tin granitoids. J. Geol. Soc. Lond. 169, 489–500. https://doi.org/10.1144/0016-76492011-107.
Seong, K.T., 1989. K/Ar mica dates for granites from the Bujang Melaka area. Bull. Geol. Soc. Malaysia 24, 79–86.
Socquet, A., Pubellier, M., 2005. Cenozoic deformation in western Yunnan (China-Myanmar border). J. Asian Earth Sci. 24, 495–515. https://doi.org/10.1016/j.jseaes.2004.03.006.
Spikings, R., Simpson, G., 2014. Rock uplift and exhumation of continental margins by the collision, accretion, and subduction of buoyant and topographically prominent oceanic crust. Tectonics 33, 1–21. https://doi.org/10.1002/2013TC003425.
Srisuriyon, K., Morley, C.K., 2014. Pull-apart development at overlapping fault tips: Oblique rifting of a cenozoic continental margin, northern mergui basin, andaman sea. Geosphere 10, 80–106. https://doi.org/10.1130/GES00926.1.
Tagami, T., RF, G., Yamada, R., Laslett, G., 1998. Revised annealing kinetics of fission tracks in zircon and geologic implications. Adv. Fission-Track Geochronol. 99–112.
Tai Seong, K., Seong, K.T., 1990. K-Ar dating of micas from granitoids in the Kuala Lumpur-Seremban area. KWAN. Bull. Geol. Soc. Malaysia 26, 77–96.
Tapponnier, P., Peltzer, G., Le Dain, A.Y., Armijo, R., Cobbold, P., 1982. Propagating extrusion tectonics in Asia: new insights from simple experiments with plasticine. Geology. https://doi.org/10.1130/0091-7613(1982)10<611:PETIAN>2.0.CO;2.
Tjia, H.D., 1998. Origin and tectonic development of Malay-Penyu-West Natuna basins. Bull. Geol. Soc. Malaysia 42, 147–160.
Upton, D.R., 1999. A Regional Fission Track Study of Thailand: Implications for Thermal History and Denudation. University of London.
Upton, D.R., Bristow, C.S., Hurford, A.J., Carter, A., 1997. Tertiary tectonic denudation in northwestern Thailand: Provisional results from apatite fission-track analysis. In: Proc. Int. Conf. Stratigr. Tecton. Evol. Southeast Asia South Pacific, pp. 421–431.
Van Hinsbergen, D.J.J., Kapp, P., Dupont-Nivet, G., Lippert, P.C., Decelles, P.G., Torsvik, T.H., 2011. Restoration of Cenozoic deformation in Asia and the size of Greater India. Tectonics 30, 1–31. https://doi.org/10.1029/2011TC002908.
Wagner, G., van den Haute, P., 1992. Fission-Track Dating. Springer, Netherlands.
Wang, G., Wan, J., Wang, E., Zheng, D., Li, F., 2008. Late Cenozoic to recent transtensional deformation across the Southern part of the Gaoligong shear zone between the Indian plate and SE margin of the Tibetan plateau and its tectonic origin. Tectonophysics 460, 1–20. https://doi.org/10.1016/j.tecto.2008.04.007.
Watkinson, I., Elders, C., Hall, R., 2008. The kinematic history of the Khlong Marui and Ranong Faults, southern Thailand. J. Struct. Geol. 30, 1554–1571. https://doi.org/10.1016/j.jsg.2008.09.001.
Watkinson, I., Elders, C., Batt, G., Jourdan, F., Hall, R., McNaughton, N.J., 2011. The timing of strike-slip shear along the Ranong and Khlong Marui faults, Thailand. J. Geophys. Res. Solid Earth 116, 1–26. https://doi.org/10.1029/2011JB008379.

Whittaker, J.M., Müller, R.D., Sdrolias, M., Heine, C., 2007. Sunda-Java trench kinematics, slab window formation and overriding plate deformation since the cretaceous. Earth Planet. Sci. Lett. 255, 445–457. https://doi.org/10.1016/j.epsl.2006.12.031.

Williams, H.H., Fowler, M., Eubank, R., 1995. Characteristics of Selected Palaeogene and Cretaceous Lacustrine Source Basins of Southeast Asia. Hydrocarb habitat Rift basins. pp. 241–282. https://doi.org/10.1144/gsl.sp.1995.080.01.12.

Williams, S.E., Whittaker, J.M., Granot, R., Müller, D.R., 2013. Early India-Australia spreading history revealed by newly detected Mesozoic magnetic anomalies in the Perth Abyssal Plain. J. Geophys. Res. Solid Earth 118, 3275–3284. https://doi.org/10.1002/jgrb.50239.

Zahirovic, S., Seton, M., Müller, R.D., Müller, R.D., 2014. The cretaceous and Cenozoic tectonic evolution of Southeast Asia. Solid Earth 5, 227–273. https://doi.org/10.5194/se-5-227-2014.

Zhang, B., Zhang, J., Zhong, D., Yang, L., Yue, Y., Yan, S., 2012. Polystage deformation of the Gaoligong metamorphic zone: Structures, 40Ar/ 39Ar mica ages, and tectonic implications. J. Struct. Geol. 37, 1–18. https://doi.org/10.1016/j.jsg.2012.02.007.